Structural problems and structures

Objekttyp: **Group**

Zeitschrift: **IABSE reports = Rapports AIPC = IVBH Berichte**

Band (Jahr): **62 (1991)**

PDF erstellt am: **23.07.2024**

Performance Assessment of Cap-Column Joints Under Seismic Loading

Evaluation de la résistance de joints pile-pont soumis aux séismes

Begutachtung von Rahmenecken unter Erdbebenbelastung

Frieder SEIBLE
Prof. of Struct. Eng.
Univ. of California, San Diego
La Jolla, CA, USA
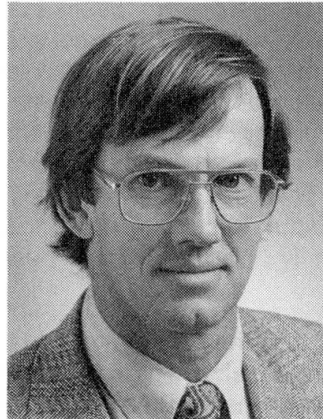
M. J. Nigel PRIESTLEY
Prof. of Struct. Eng.
Univ. of California, San Diego
La Jolla, CA, USA
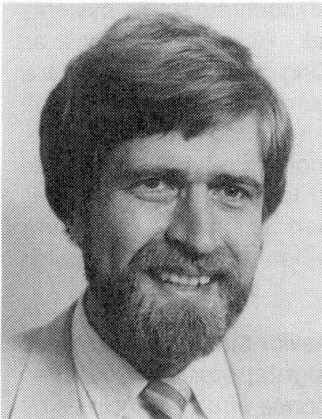
Frieder Seible has been a member of the UCSD faculty for 7 years. He has Civil Engineering degrees from Germany, Canada and the USA and his research combines large scale experimental testing and non-linear analystical modeling of structural concrete systems.

M.J. Nigel Priestley has received numerous international awards (ACI, PCI) for his earthquake engineering and structural concrete research contributions. He was a member of the faculty of the University of Canterbury, Christchurch, New Zealand for eleven years prior to joining UCSD.

SUMMARY

An overview of joint damage in beam-column joints of multi-level bridge bents during the 1989 Loma Prieta earthquake, is presented. Assessment criteria for evaluating seismic performance characteristics and retrofitting schemes for existing concrete bridge structures, are developed. The application of analytical concrete models of various complexities in support of structural concrete design is demonstrated.

RÉSUMÉ

On présente ici une vue d'ensemble des dommages causés aux angles des cadres soutenant des ponts multi-niveaux, advenus lors du tremblement de terre de Loma Prieta en 1989. Les critéres d'évaluation de base concernant l'estimation des caractéristiques de résistance aux séismes et les possibilités de renforcement des ponts existants sont développés; à cet effet, l'application de modèles analytiques de divers niveaux de difficulté servant de support au dimensionnement des structures en béton armé est démontrée.

ZUSAMMENFASSUNG

Über Schäden in Knotenpunkten von Balken-Stützenverbindungen in mehrstöckigen Brücken-rahmen während des Loma Prieta Erdbebens von 1989 wird ein Überblick gegeben. Beurteilungs-kriterien für die Begutachtung und Einschätzung des Erdbebenverhaltens und der Verstärkung von bestehenden Betonbrücken werden aufgezeigt. Die Anwendung von analytischen Modellen im konstruktiven Betonbau von unterschiedlicher Komplexität wird demonstriert.

1. INTRODUCTION

The Loma Prieta (San Francisco) earthquake of October 17, 1989 reemphasized the vulnerability of structural concrete systems to cyclic displacements resulting from seismic attack. The dramatic collapse of a one-mile section of the Cypress Viaduct in Oakland can be traced to inadequate performance of the cap-column joint region in the supporting bents of the elevated bridge structure. Investigation of the joint reinforcement showed inadequate structural detailing of the joint region for the encountered seismic force levels. While the Cypress collapse was well publicized in the press and technical literature, only limited information can be found on similar structural joint damage to other elevated roadways in the San Francisco–Oakland Bay Area, see Fig. 1, which led to the temporary or permanent closure of several major freeway arteries including the Embarcadero Viaduct (I-480), the China Basin/Southern Freeway Viaduct (I-280) and the Central Viaduct (Highway 101) in San Francisco, as well as the Southbound Connector (I-980) in Oakland [1].

While most of these bridge sections were designed and built in the 1950's and 1960's, some of them were completed as late as 1985. This raises questions concerning not only past but current detailing practice for structural concrete joints. Design rules for beam and column members of structural concrete frame systems seem to be widely accepted and standardized in similar form around the world. However, as soon as aspect ratios of structural members approach unity, design guidelines and supporting design models show a wide range of different approaches. Limited detailed design models for these regions exist when full three-dimensional force transfer of axial, flexural and torsional structural action is required simultaneously. Also, most design models focus on single monotonic structural loading and do not address fully reversed cyclic loading patterns. Thus, the question arises whether a unified approach for design and analysis models in support of structural concrete detailing exists or if the state-of-the-art in structural concrete detailing still relies primarily on experience to design and detail complex members for realistic loading conditions.

Both analytical models to study the in-depth mechanism of structural concrete behavior through various limit states and design models developed to unify the structural detailing and design approach have seen comprehensive recent developments. In a direct extension of early structural concrete design principles by Ritter (1899) and Mörsch (1909), Schlaich et al. have developed a comprehensive design approach toward structural concrete detailing which ensures internal force transfer through discrete compression and tension (strut and tie) members, satisfying equilibrium by simple truss mechanisms [2]. This approach has become a powerful design tool since it allows a variety of detailing solutions as long as basic anchorage and stress limit states are observed, but most importantly it allows and forces the design engineer to develop a consistent design model resulting in an engineered solution rather than in a design resulting from a recipe application. Problems and limitations arise when design solutions based on inappropriate truss mechanisms are attempted and when the discrete member forces are of magnitudes which cause stress limit and anchorage problems and thus require a distributed or smeared approach. Parallel to the consistent strut and tie model development, Collins et al. developed the juxtaposed position of a smeared or distributed behavior model [3], which is based on homogeneous behavior of structural concrete even in its cracked state and resulting orthogonal principal compression and/or tension fields of the internal forces. Based on mechanical principles of an orthotropic homogeneous material, the orientation of the resulting stress fields is derived from compatibility and equilibrium conditions. The resulting stress fields are subsequently discretized in concrete and reinforcement action which forms the basis for a rational structural concrete design approach. Similar to the discrete strut and tie model, additional considerations for anchorage and local concentrated force transfer are required and limitations exist where either reinforcement is heavily concentrated rather than distributed, and where structural action results in a few large cracks rather than in the ideal distributed (smeared) crack pattern. Thus, while both design models are different in the approach, they are rather complementary in the overall design process, especially when in addition to the force transfer in the joint or member, deformation limit states also need to be considered.

Both of the above models provide comprehensive design approaches to structural concrete detailing but are fully applicable only when simple monotonic loading conditions exist up to design levels with sufficient margin to the ultimate limit state. Where deteriorating bond phenomena along the reinforcement, opening and closing of cracks under reversed cyclic loading, deterioration of concrete contribution in developing local failure mechanisms, and the development of ductile hinges (which incorporate all of the above aspects) are present, the above models may not be adequate and additional considerations to both design

approaches are needed as outlined by Paulay et al. for structural concrete joints under seismic action [4]. It will be shown in the following that, with these additional considerations, the above design models can also be directly applied toward the design of retrofit measures of existing critical structural concrete regions as found in the San Francisco double-deck freeways. Further, it will be shown that complete failure sequences and limit states of these structural systems can be traced using advanced nonlinear analytical structural concrete models.

The critical role of structural concrete joints in beam-column systems and their behavior under seismic loading is evaluated in this paper on the example of joint performance in elevated bridge structures during the Loma Prieta earthquake and the applicability of various design and analysis models to the structural concrete joint problem is demonstrated, both for the assessment of joint performance during the earthquake and subsequent repair and retrofit strategies.

2. SEISMIC PERFORMANCE ASSESSMENT

2.1 General Assessment Approach

To assess the expected seismic performance of structural concrete beam column joints, it is important that the joint under consideration is evaluated in direct relationship to the actual adjacent member capacities. This requires a state or capacity determination of adjacent beams and columns with consideration of (1) actual material properties at the time of evaluation, i.e., probable concrete strength, not the design strength $\sqrt{f'_c}$, actual stress strain behavior for the reinforcement not nominal specified design yield levels, (2) proper consideration of axial load effects, (3) proper consideration of possible confinement effects from transverse reinforcement, (4) reduced concrete shear contribution in areas of large fully reversed cyclic deformation, and (5) realistic bond and anchorage estimates particularly for large diameter reinforcing bars.

A preliminary performance assessment of joints comprises the following steps: *Step I:* Realistic member capacities based on the above considerations are derived for both flexure and shear, and the critical failure mechanism is determined by direct comparison of the shear capacity with the plastic flexural limit state shear V_p derived from the appropriate flexural plastic hinge failure model of the member. If V_p is larger than the calculated shear capacity, a potentially brittle shear failure can be expected without the formation of ductile flexural plastic hinge mechanisms. *Step II:* Based on the possible member failure mechanisms, the expected global collapse mechanism for the complete structural system is derived by comparing combined dead load and lateral seismic force action with the derived capacities. *Step III:* From the identified systems collapse mechanism, critical joint forces can now be determined at the collapse state and a direct comparison with most probable joint capacities will indicate if joint distress degrades the capacity of the collapse mechanism or if the joint behaves as ideally assumed within or close to the elastic range. *Step IV:* Finally, equivalent seismic base shear forces are estimated corresponding to the lateral force level which causes collapse based on the above failure mechanism. Excessive joint distress can lead to a reduction of this base shear coefficient, particularly when a large number of cyclic load reversals and the associated joint degradation is considered.

Application of the above preliminary seismic assessment procedure to the San Francisco double-deck bridge bents has shown that the joints did not meet design criteria for earthquake resistant ductile structures summarized by Paulay et al. [4] as: (1) joint strength should exceed the maximum strength of the weakest connecting member, (2) structure capacity should not be jeopardized by strength degradation in the joint, and (3) joint response should be elastic during moderate seismic disturbances.

The preliminary joint behavior assessment outlined above can be supplemented and refined by more detailed analysis and design models as demonstrated in the following for one specific case study performed following the 1989 Loma Prieta earthquake.

2.2 The Oakland Southbound Connector, I-980, Bent 38

A single-deck outrigger bent (bent #38) with only a 0.92 m (3 ft) outrigger cap beam extension past the superstructure on I-980 featured heavy joint damage as shown in Fig. 1c,d,e. Built in 1985, the column was well confined with an interlocking spiral, see Fig. 3, however, this spiral did not continue into the joint region

where it was replaced by a 5 gauge wire spiral with D = 5 mm at 10 cm (ϕ 0.2 in. @ 4 in.). Also, the cap beam reinforcement, aside from the top and bottom bars, see Fig. 3, did not extend into the joint region.

A capacity check on the cap beam and column capacities showed that the cap beam capacity is critical for positive moment due to the insufficient anchorage length of 1.8 m (72 in.) for the D = 57 mm (#18) bars which, based on ACI 318-89, require a basic development length of 3.0 m (117 in.) which is likely to be on the conservative side. In the other loading direction (negative moment in the joint), the column capacity is critical. Joint shear force levels derived from simple stress models, Fig. 4, show joint shear stress levels of $0.37\sqrt{f'_c}$ MPa ($4.3\sqrt{f'_c}$ psi) and $0.5\sqrt{f'_c}$ MPa ($6.0\sqrt{f'_c}$ psi), under positive and negative moment loading, respectively, which are both above an assumed level of $0.33\sqrt{f'_c}$ MPa ($4.0\sqrt{f'_c}$ psi), where diagonal tension cracking in the joint can be expected. Since the shear capacity of the 5 gauge wire spirals does not add significant joint shear capacity, the formation of any flexural hinge mechanism in adjacent members was inhibited.. This explains the encountered diagonal joint crack patterns during the Loma Prieta earthquake, see Fig. 1c,d,e.

In addition to the diagonal crack patterns, large areas of cover concrete spalling along the outer cap corner as well as a ruptured D = 57 mm (#18) reinforcement bar which was bent on a 45 cm (1'-6") radius were observed, see Fig. 1d,e.

The first phenomenon of cover concrete spalling can be explained with the fully reversed cyclic loading. Under negative moment, flexural cracks open on the cap surface as shown in Fig. 3 and under subsequent positive moment loading, the entire compression force has to be transferred through the negative moment reinforcement until the cracks can close. These high compression forces in the negative moment reinforcement transferred to the concrete by bond, have a tendency to spall off the concrete cover between flexural cracks developed in the previous tensile excursions. The second phenomenon, the ruptured reinforcing bar, see Fig. 1d, points to a potentially critical problem which needs further investigation. Common ultimate strain levels in D = 57 mm (#18) f_y = 414 MPa (Grade 60) bars are in a range from 7 to 15%. Introducing a R = 45 cm (18 in.) radius bent into a D = 57 mm (#18 or ϕ = 2.25 in.) bar causes strain levels of D/(2R) = 225/(2 × 18) = 6.25%, which is close to the ultimate strain range. The very low strain reserves and possible strain aging effects which raise the notch ductile temperature at which steel will fail in a brittle mode can cause sudden failure in these bent bars at very low additional strain levels.

In addition to the simple stress models of the knee bent joint, detailed nonlinear finite element simulations, see Fig. 2, based on extended compression field principles were performed to determine analytically failure modes and joint deformation contributions to the overall bent deformations. Reinforcement development of straight bars was modeled by assuming a reduced yield level in the anchor zone decreasing linearly from the full yield at the ACI 318-89 basic development location to zero at the bar end. Subsequently derived yield patterns in bar anchorage regions therefore are indicative of bond failure or slip. Superimposed to the dead load case, the half bent, Fig. 2, was subjected to lateral force, and force-deformation envelopes with major event indicators, depicted for positive moment loading in Fig. 5, were obtained. Associated crack, slip/yield and first crushing patterns, see Fig. 5, indicate the failure mechanisms in the joint region. The heavy yield in the joint center, both horizontally and vertically, indicates the deficiency of both vertical and horizontal joint shear reinforcement, particularly under negative moment on the joint. Also, the crushing of the concrete in the outer joint region under the bent negative moment reinforcement under loading to the left or negative moment indicates the high compressive stress state and associated transverse prying forces in this region and the need for sufficient transverse confinement reinforcement, as outlined by Schlaich et al. [2], for strut and tie models for negative moment knee joints.

Since joints should be detailed based on capacity considerations such that the major inelastic action occurs in the cap or column, and since they should remain effectively elastic for small seismic disturbances (Paulay et al. [4]), the nonlinear finite element analysis was repeated with a linear elastic joint for a direct comparison of deformation limit states. As can be seen from Fig. 5, while joint deformations did not contribute significantly to the initial overall structural deformations, the failure mode in the positive moment direction shows improved ductile behavior when the failure mechanism is shifted from joint distress to flexural cap beam hinging. It should be noted that the cap beam capacity still may be artificially low due to the reduced yield strength in the bottom D = 57 mm (#18) reinforcing bars based on a reduced development length according to ACI 318-89. Negative moment loading behavior is also improved by forcing the yield mechanism clearly into the column (not shown). Since the bent joint failure is the critical link in the overall behavior, repair/retrofit of these joints is a logical next step.

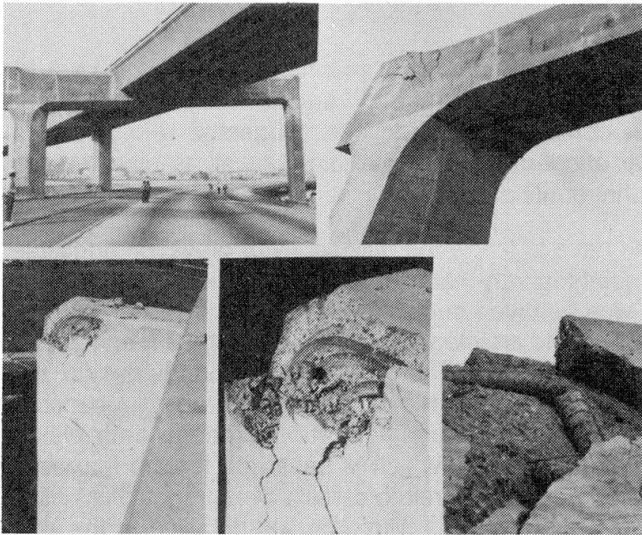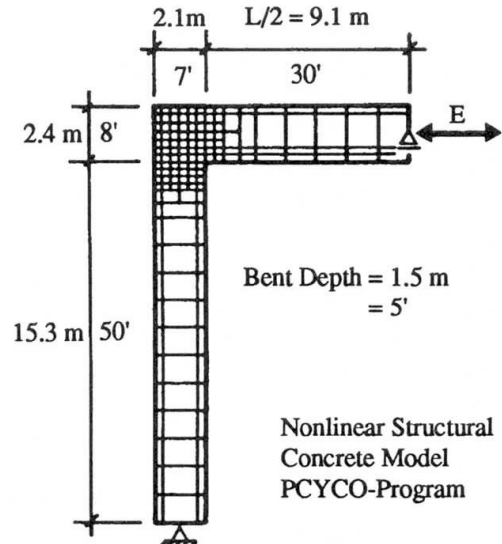**Fig. 1** Outrigger bent joint damage
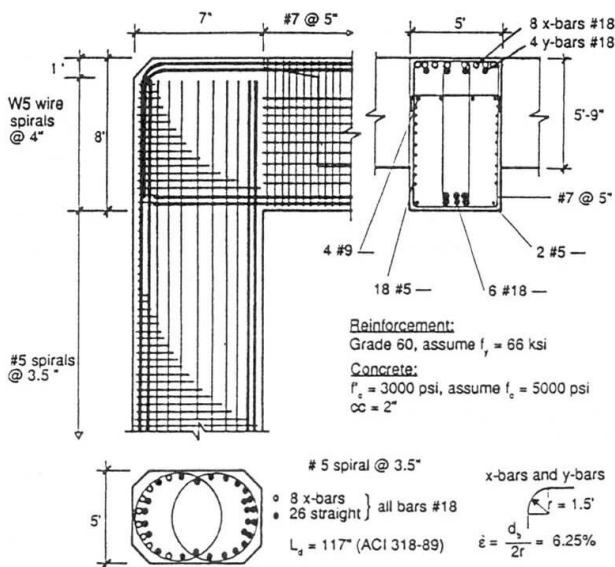

Fig. 2 Analytical bent model

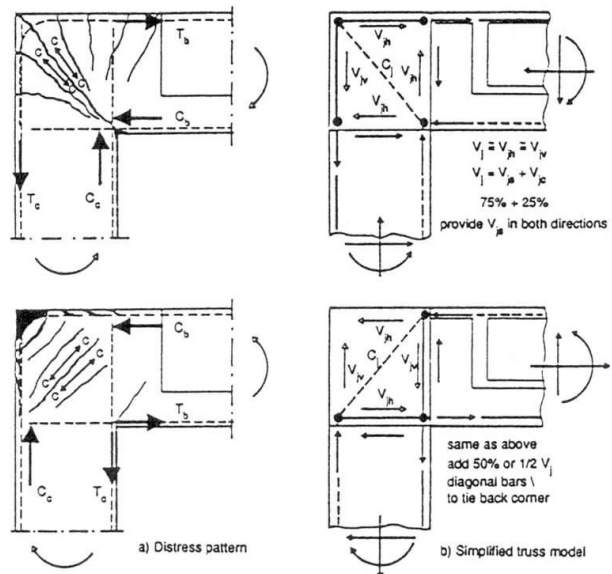**Fig. 3** I-980, #38, Reinforcement details
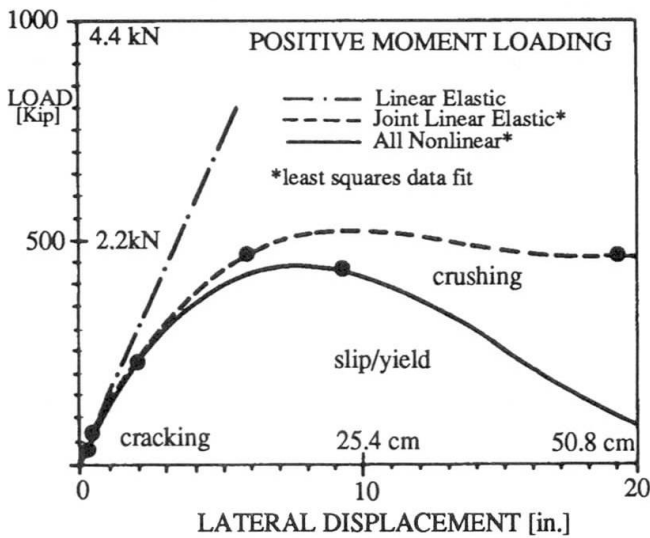

Fig. 4 Joint behavior models
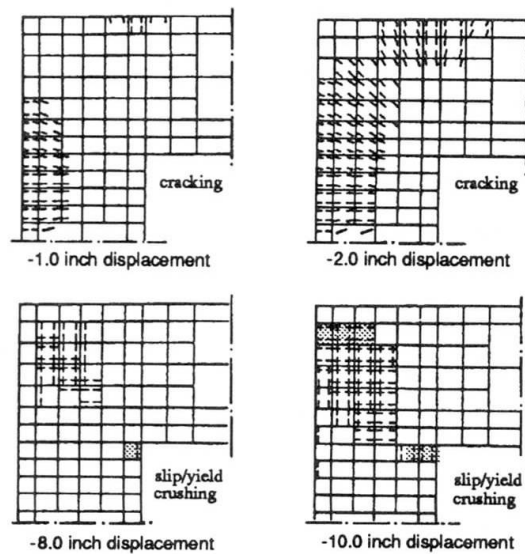

Fig. 5 Positive moment limit states

Fig. 6 Negative moment distress patterns

3. REPAIR AND RETROFIT

Cap/column joints in elevated roadways are probably the most difficult members in a bridge bent to successfully repair and/or retrofit for seismic loading. Both horizontal and vertical heavy reinforcement patterns from cap beams and columns provide for complex geometric and congested reinforcement patterns in the joint. Also, the critical aspects of bar anchorage within the joint as well as plastic hinge development directly adjacent to the joint complicate the retrofit design.

Criteria for seismic retrofit design of cap/column joints have to follow the philosophy of providing a reliable ductile structural system. Since ductility within the joints is very hard to achieve, the joint retrofitting is geared toward the formation of clearly defined and well behaved ductile plastic hinges in either the cap beam or the column. In many bridge decks, the cap beam is an integral component of the superstructure which would make post-earthquake repair in this member difficult. Thus, frequently in bridge design, the ductile framing system is provided by reliable column hinges. For the retrofit design, again a capacity design approach should be employed which ensures in the case of the joint retrofit predominantly elastic behavior of the joint region. This can be achieved by joint design which is based on factored nominal column design moments, e.g., $1.5 \times M_n$, where the factor accounts for reinforcement overstrength, including strain hardening, confinement effects and concrete strength increase with time. In detailing of the joint repair retrofit, the congested reinforcement layout within the joint as well as high nominal joint shear stress levels typically require an increase in size of the joint region.

Detailing for repair or retrofit of the damaged knee joint on I-980, bent #38, can be derived using either strut and tie models as outlined in Fig. 3 with additional considerations as outlined in [2] for transverse splitting under negative moment and tie back for fully reversed cyclic loading, or directly from the force states derived from the compression field analysis, see Fig. 5. A possible repair measure consists of providing an additional 23 cm (9 in.) concrete jacket around the existing joint with horizontal and vertical distributed joint reinforcement and a diagonal corner tie back based on force and reinforcement quantities derived in Fig. 4. The damaged joint concrete can either be removed and the joint rebuilt completely or the damaged joint can be epoxy injected subsequent to removal of loose concrete, roughening of the interface, and adequate doweling bonding of the added structural concrete jacket.

4. CONCLUSIONS

The assessment of beam-column joint performance during the 1989 Loma Prieta earthquake has shown that compression field based analysis and design models are invaluable tools to investigate existing capacities, failure modes, and deformation limit states. Strut and tie models are particularly suited for design of new joints and retrofit and repair measures. However, in capacity assessment, where dependence on distributed concrete tensile stresses is essential and where bond forces cause distributed shear input, the basic strut and tie model is limited. The detailing of structural concrete joints subjected to fully reversed cyclic loading requires additional design detailing considerations which account for opening and closing of large flexural cracks and the associated compression force transfer through the reinforcement. Due to the large column height, the joint deterioration was shown to contribute insignificantly to the initial structural deformation, while non-ductile joint failure resulted in substantially reduced ultimate deformation capacities.

REFERENCES

[1]   PRIESTLEY M.J.N. and SEIBLE F., Assessment of Bridge Damage During the Loma Prieta Earthquake. Structural Systems Research Project, Report No. SSRP-90/01, March 1990.

[2]   SCHLAICH J. and SCHÄFER K., Konstruieren im Stahlbetonbau. Betonkalender 1989, Verlag Ernst & Sohn, pp. 563-715.

[3]   COLLINS M.P., Towards a Rational Theory for RC Members in Shear. ASCE Journal of the Structural Division, Vol 104, April 1978, pp. 649-666.

[4]   PAULAY T., PARK R. and PRIESTLEY M.J.N., Reinforced Concrete Beam-Column Joints under Seismic Actions. ACI Journal, Vol. 75, No. 11, November 1978, pp. 585-593.
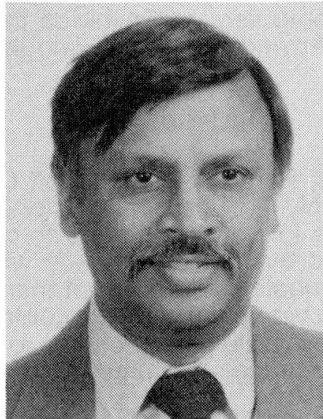
Finite Element Modelling for Analysis of Highly Skewed Bridges

Analyse par éléments finis de ponts à dalles fortement biaises

Finite-Element-Analyse von stark gekrümmten Brücken

Seetha V. RAMAIAH
Prof. Associate
Parsons Brinckerhoff Quade & Douglas
Tempe, AZ, USA

Seetha V. Ramaiah graduated in civil engineering from the University of Mysore in 1958. His experience as a consulting engineer includes several major bridge projects both in Canada and the USA, including the award winning 7th Street Bridge, an hourglass shaped urban interchange structure in Phoenix, AZ.

SUMMARY

Background, reasons for use, and some results of the finte-element method of analysis are presented by the author. The main features of the study are skew bending effects; torsional moments, shears and support reactions; and large reactions caused by post-tensioning forces.

RÉSUMÉ

L'auteur présente la documentation, la justification ainsi que les résultats de la méthode par éléments finis appliquée; les principales caractéristiques de l'étude sont les effets des flexions biaises, les moments de torsion, cisaillement et réactions d'appui, ainsi que les réactions significatives causées par la précontrainte.

ZUSAMMENFASSUNG

Der Hintergrund und die Ursachen und Ergebnisse der Finiten-Elemente-Methode werden präsentiert. Die wichtigsten Punkte der Untersuchung sind: schiefe Biegung, Torsionsmomente, Querkräfte und Auflagerkräfte, sowie grosse Auflagerkräfte infolge Vorspannung.

1.   INTRODUCTION

1.1   Background

The behavior of skewed bridges has ben a pre-occupation of structural engineers for decades. Traditionally skewed bridges were analyzed and designed considering the longest length between the supports as the actual span length. Conventional wisdom assumed that such a conservative approach would result in a very safe design. The means or methods to do a more exact analysis did not exist until the advent of computers. The computers gave the engineers the opportunity to use more refined methods of analysis like the grid and space frame analysis to study the behavior of skewed bridges. The more exact methods of analysis like the "finite element method of analysis" were time consuming and needed large computers. The arrival of the newer, faster and larger computers has avoided this limitation and finally given engineers the means to analyze highly skewed box girder bridges within a reasonable budget and time frame.

1.2   Purpose and Objectives

During the last couple of years, Parsons Brinckerhoff Quade & Douglas, Inc. (PBQ&D) had to analyze and design several highly skewed post-tensioned box girder bridges. The skew angles on these bridges varied from a low of 43 degrees to a high of 70 degrees. The unavoidable high skew angles forced us to evaluate and verify whether the results of the finite element method of analysis would be substantially different than conventional methods or approximate methods. The objective of this whole effort was to obtain realistic behavior of these structures and to examine the local as well as global effects of external and internal loads on these bridges and assure the integrity of the structures.

2.   SKEW BENDING

2.1   Cause of Skew Bending

In any bridge, the principal bending occurs along the shortest axis between the supports, which happens to be perpendicular to the axis of supports. In a non-skewed bridge the supports are along the transverse axis which is perpendicular to the longitudinal axis of the bridge. The principal bending of the girders and the whole structure occurs about the transverse axis parallel to the supports, along the longitudinal axis. This behavior has always dictated the direction of the girders in a concrete box girder bridge to be parallel to the longitudinal axis.

In a skewed bridge, the supports are not along the transverse axis. They are located along an axis skewed to the transverse axis of the bridge. The longitudinal axis of the bridge remains the same. The principal bending occurs about an axis parallel to supports along a new longitudinal bending axis which is perpendicular to the supports. This new longitudinal bending axis is skewed to the longitudinal axis of the bridge and is almost parallel to the shortest distance between the supports. The principle bending of the structure along this new longitudinal bending axis is called skew bending and its effects caused in a skewed bridge are referred to as skew bending effects. These effects must be carried by the girders or webs, by resolving them along the longitudinal and transverse axis of the structure.

2.2   Effects of Skew Bending

The principal bending moment along the new longitudinal bending axis is resolved to a bending moment along the longitudinal axis of the structure and a torsional moment about the longitudinal axis. The torsional moments caused by skew bending effects, in turn, cause an uneven distribution of horizontal and vertical shears at a section normal to the longitudinal axis of the bridge. This uneven distribution of horizontal and vertical shears, affects the location of maximum moments, produces large variations in support reactions and the post-tensioning forces which are normally negligible in a non-skewed bridge result in uplifts at certain supports

Five highly skewed bridges included in the three bridge sites listed below were part of the Aviation Project in Tucson Arizona and are the subject of this paper.

3.   METHODS OF ANALYSIS AND PROGRAMS EVALUATED

Three dimensional grid, plane frame with charts for increased shears and finite element method of analysis were evaluated for the reliability of results. Programs considered were CALTRAN Bridge Memo (Reference 1) for Designers 15-1, Cell4 Program (Reference 2), MDC STRUDL Program (Reference 3) and the 3-Dimensional Grid Analysis Program (Reference 4).

The CELL4 program was selected for use in view of the savings offered in modelling, computer time, ease of obtaining sectional forces, moments and automatic generation of equivalent loads for post-tensioning forces. In order to ascertain and validate the results of CELL4 program two identical models were tested using CELL4 and STRUDL programs (Figures 1 and 2). The differences between results of the two models though not exactly the same were within reasonable limits of accuracy required for design. The maximum stresses, moments and deflections were within 5% of each other. The STRUDL model in Figure 2 has a thicker pier diaphragm than the CELL4 model, which accounts for some of the differences in the reactions. The only results that have a wide variation are the two uplift reactions at the acute corners.

The closeness of results from both the programs gave us sufficient confidence to use CELL4 on all bridges except the Council/Toole Avenue bridge, which has a variable depth.

4.   DISCUSSION OF MODELS

4.1   S.P.R.R. Bridge (Figures 3 and 4)

In order to increase the accuracy of the results in the finite element analysis, the aspect ratio of the elements was kept to 1 in critical areas and to 2 in non critical areas. The finite element model for this structure has 1428 joints and 1818 elements.

4.2   Council/Toole Avenue Bridges (Figures 6 and 7)

The finite element used is called "SIPQ", a quadrilateral curved element with four corner nodes and four midside nodes with five degrees of freedom (DOF). The aspect ratio varied from 1 to 2 depending on the geometry and the importance of certain critical areas. This model had a total of 1482 elements and 4119 joints.

4.3   Euclid/Park Structures (Figure 8)

PBQ&D was involved in the review of final design for these two structures. The design was based on a 3-dimensional grid analysis. CELL4 program was used for the design verification. The finite element model consisted of 1,116 joints; and 1,370 elements. The aspect ratio of elements was 1 in critical areas and 2 in less critical areas.

5.   DISCUSSION OF RESULTS

5.1   DL Reactions (Figures 3, 6 and 8)

The reactions do not follow the normal pattern given by other conventional methods of analysis. The higher reactions seem to occur at supports that lie very close to the principal longitudinal bending axis, illustrating the skew bending effects. At certain locations, supports reactions vary by 100%.

5.2   Reactions Due to Post-Tensioning Force (Figures 5, 6, and 8)

Normally one does not expect any significant reactions due to internal equivalent loads due to post-tensioning force. The results show this is apparently not the case. We attribute this to the heavy torsional moments caused by the skew bending effect.
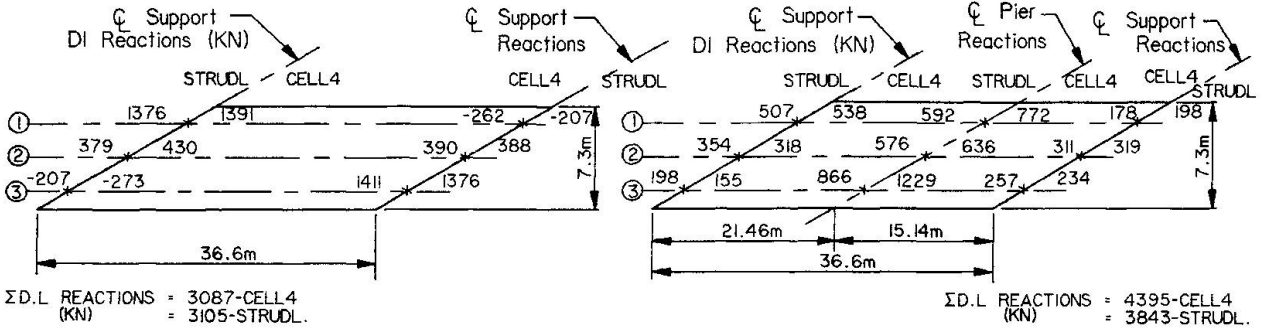
Fig. 1   Single Span TEST Model
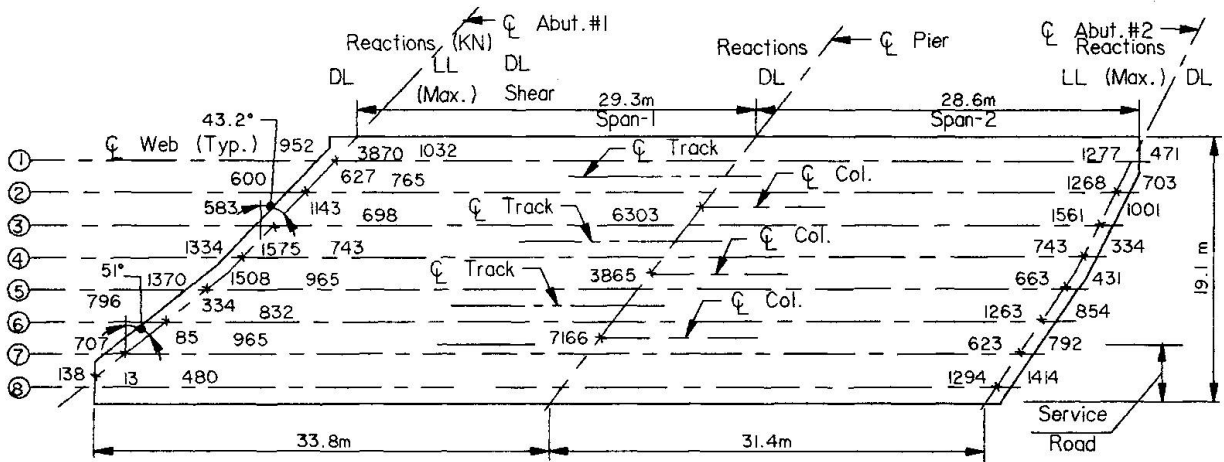
Fig. 2   Two Span TEST Model

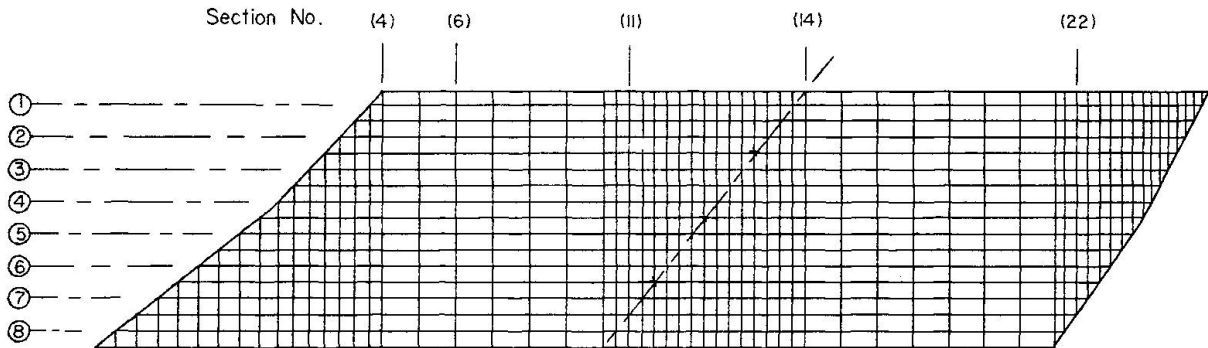Fig. 3   Sectional Framing Plan With Support Reactions - SPRR Bridge

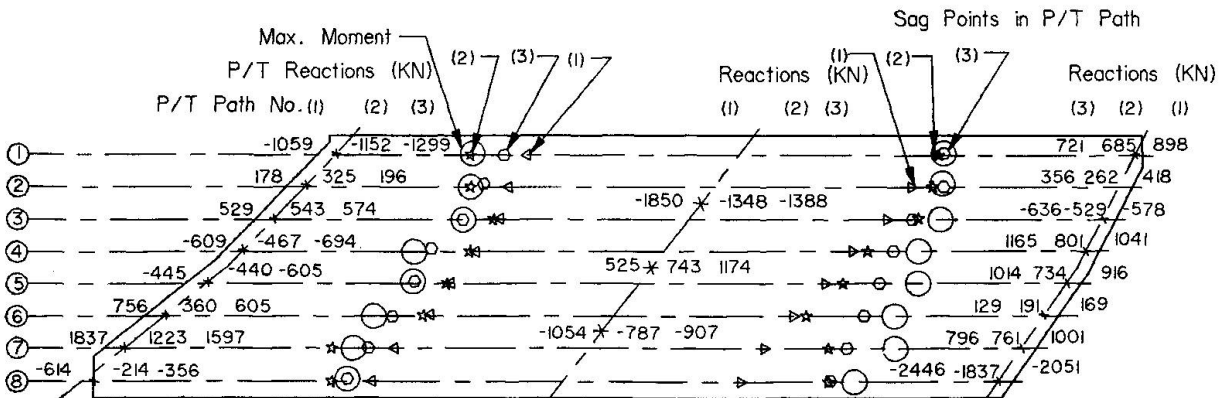Fig. 4   Finite Element Discretization Mesh - SPRR Bridge

Fig. 5   Post-Tension Reactions (KN), Points of Max. Moments and
Sag Points in Tendon Paths - SPRR Bridge

Table I   Section Torsional Moment and Shear for SPRR Bridge

| SECTION	4		6		II		I4		22	
	Torsion	Shear	Torsion	Shear	Torsion	Shear	Torsion	Shear	Torsion	Shear
DL	-16592	-1112	-16357	672	319	3287	-12496	-4435	-10527	2393
DL+SDL	-25397	-1841	-23780	747	1588	4839	-20283	-6610	-13049	3363
DL+SDL+LL	-52597	-4537	-42440	-98	5109	7446	-16686	-7135	-9731	2953
P_j =17392 Path I	23495	3443	29787	654	-14261	-7250	34247	9212	16934	-4497
P_j =15657 Path 2	30335	3269	35683	-476	-10893	-7602	17848	8558	20269	-4822
P_j =15657 Path 3	27086	2896	33311	-267	-13887	-7272	21300	8674	20265	-4492

Units Are KN-m and KN
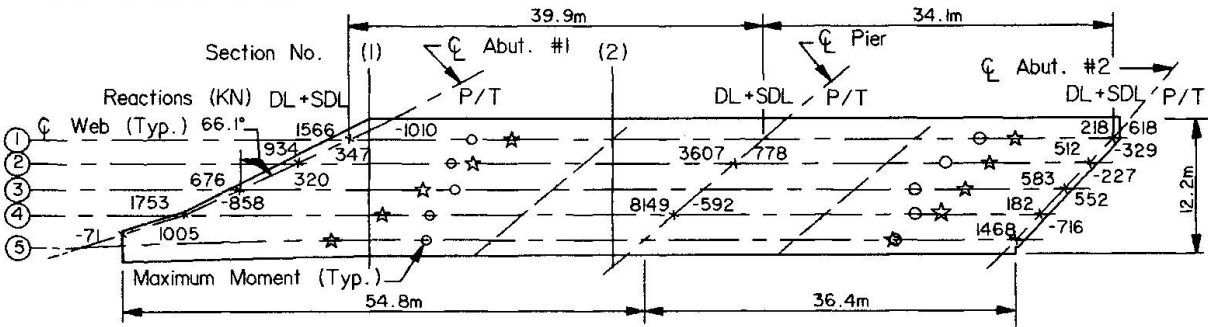
Fig. 6   Sectional Framing Plan for EB Council/Toole Ave. Bridge
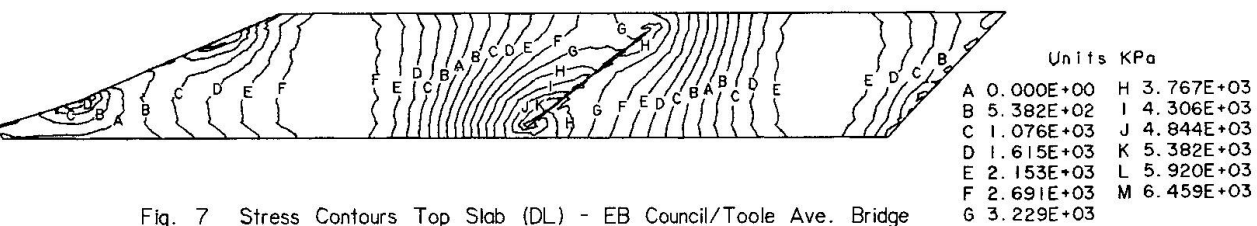(DL+SDL) And P/T Reactions.

ΣP/T Reaction = -112 (KN)

o   Points of
     Max. Moments

☆   Sag Points
     In P/T Path

Units KPa

A 0.000E+00   H 3.767E+03
B 5.382E+02   I 4.306E+03
C 1.076E+03   J 4.844E+03
D 1.615E+03   K 5.382E+03
E 2.153E+03   L 5.920E+03
F 2.691E+03   M 6.459E+03
G 3.229E+03

Fig. 7   Stress Contours Top Slab (DL) - EB Council/Toole Ave. Bridge
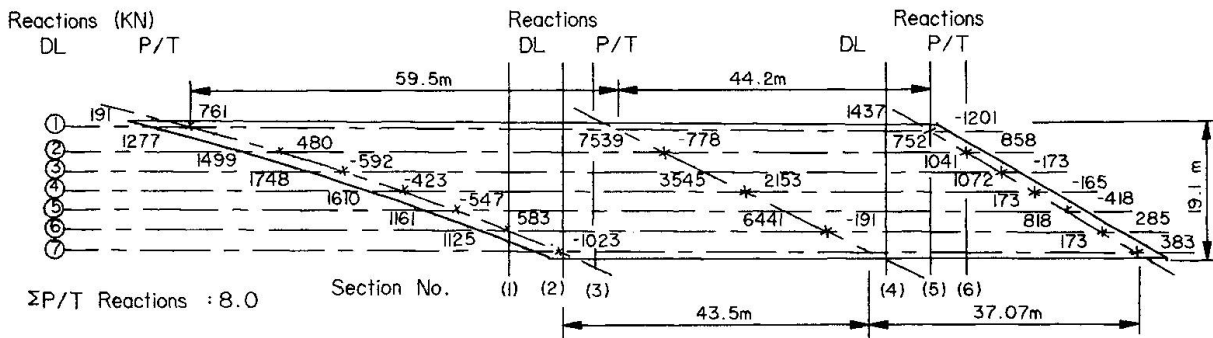
ΣP/T Reactions : 8.0

Fig. 8   Sectional Framing Plan With Support Reactions for Euclid/Park Ave. Bridge

Table 2   Torsional Moments
for EB Council/Toole Ave. Bridge

SECTION	I	2
DL	-9994	-10285
DL+SDL	-12430	-12794
DL+SDL+LL	-15679	-16127
P/T	8421	6772

Units Are KN-m

Table 3   Section Torsional Moments for WB Euclid/Park Ave. Bridge

SECTION	I	2	3	4	5	6
	Torsion	Torsion	Torsion	Torsion	Torsion	Torsion
DL	14428	29599	29793	22793	22581	9607
DL+SDL	17208	35335	35539	26984	26790	11286
DL+SDL+LL	20877	42977	42893	33090	33082	13999
P/T	-15286	-31720	-23184	-18090	-25717	-11309

Units Are KN-m

5.3   Points of Maximum Moment (Figures 5 and 6)

In a two span highway bridge with no skews and simple supports at each end, the points of maximum moment would be located usually at 0.4 of the span from the exterior abutment support. The points of maximum moment in the SPRR bridge vary from 32 percent in girders 1 and 2 to 54 percent in girder 8 in span 1. This is reversed in span 2 and the points of maximum moment vary from 48 percent in girder 1 and 2 to 32 percent in girders 7 and 8.

The fluctuations in the location of points of maximum moments in the Council/Toole Avenue bridges are very large. The distance from the center of abutment to these points varies from 25 percent of span at girder 1 to 55 percent at girder 5. The support reactions are more than 100 percent different at certain locations. Note the heavy reactions at the top left hand corner and the bottom right hand corner supports. The line joining these points, almost coincides with one of pier supports. Though it is not perpendicular to the lines of support, it seems to act like the principal longitudinal axis of the structure. The reaction of this pier is more than twice the reaction at the other pier and greatly affects the design of the cantilever pier diaphragm.

5.4   Torsional Moments (Tables 1, 2 and 3)

The Tables 1, 2 and 3 illustrate the magnitude of torsional moments induced due to the skew bending effect. Torsion steel was required for all five bridges as per references (5), (6).

6.   CONCLUSIONS AND RECOMMENDATIONS

Analysis and design of skewed bridges requires careful evaluation of skew-bending effects. Three dimensional grid analysis does not give a true account of the behavior of the skewed structure. The results are very sensitive to the torsional rigidity of the members assumed in a grid model and the comfort level for dependability of results is low.

Finite element models, with proper aspect ratios, provide the best means to evaluate the behavior of skewed bridges. Intermediate diaphragms do not have any noticeable effect on the behavior or the re-distribution of loads in a skewed box girder.

Support reactions are unpredictable by conventional procedures. Torsional moments induced by the skew need to be addressed in the design. The torsion capacity of the post-tensioned concrete box girders was not adequate to resist the total torsions induced on the structures.

The load balancing procedure does not offset all the skew bending effects in a post-tensioned concrete structure. The post-tensioning force required for load balancing is much higher than what is required for balancing the stresses.

It seems imperative that structures with skews greater than 25 degrees should be analyzed by an exact method of analysis like finite element methodology to assure the structural design integrity.

REFERENCES

1.   California Department of Transportation (CALTRANS). Bridge memo to designers 15-1, Sacramento, California, January 1986.

2.   A.C. Scordelis, E.C. Chan, M.A. Ketchum, D.D. Van Der Walt; Computer programs for prestressed concrete bridges, Department of Civil Engineering, University of California, Berkeley, march 1985.

3.   Macdonald Douglas: MDC STRUDL program, release 5.4, Oct. 1986, Saint Louis Missouri.

4.   Edmund C. Hambly: Bridge Deck Behavior, Chapman and Hall, London, 1976.

5.   Thomas T.C. HSU: Torsion of Reinforced Concrete, Van Nostrand Reinhold Company, New York, 1984.

6.   ACI: Analysis of Structural Systems for Torsion, ACI publication SP-35.
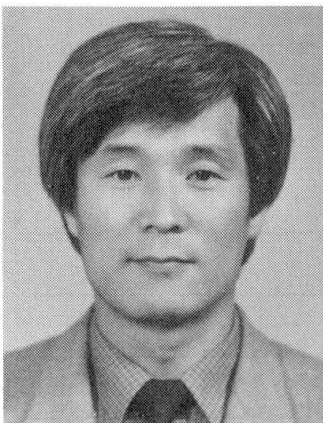
Behaviour of Prestressed Concrete Bridges Considering Construction Stages

Comportement de ponts précontraints en fonction des étapes de construction

Verhalten von Spannbetonbrücken unter Berücksichtigung des Bauzustandes
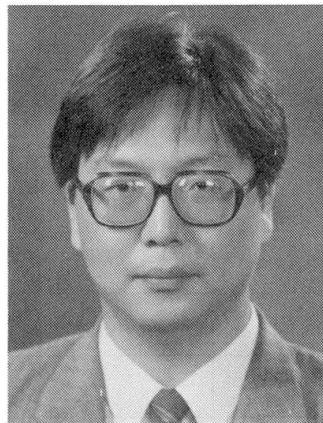
Sung Pil CHANG
Prof. of Civil Eng.
Nat. Univ.
Seoul, Korea

S.P. Chang, born 1943, obtained his Ph.D. degree at University Stuttgart. Besides teaching, he has been involved in many bridge construction projects of the Korean government.

Woo Jong KIM
Consult. Eng.
Sam Woo Eng. Co. Ltd
Seoul, Korea

W.J. Kim, born 1959, obtained his Ph.D. degree at Seoul National University in 1990. He has worked in the structural design part of a consulting firm where he is responsible for detailed design of bridges.

SUMMARY

A numerical procedure is presented for 3-dimensional prestressed concrete frame structures with stay cables considering construction stages. A finite element type is developed including the warping and flexural-torsional effects of arbitrary cross sections. The geometric nonlinear analysis during construction and linear dynamic analysis at any construction stage are incorporated. The ultimate load of the structure is not studied. The effects of creep, shrinkage and prestressing are considered by nonconservative equivalent loads.

RÉSUMÉ

Une procédure numérique est présentée dans le cas de cadres tri-dimensionnels à haubans avec prise en compte des étapes de construction. Une procédure basée sur les éléments finis est développée; elle tient compte des effets de gauchissement et de torsion-flexion de certaines sections-types. L'analyse géométrique non-linéaire effectuée durant la construction, ainsi que l'analyse dynamique linéaire y sont également incluses. Le charge ultime de la structure n'est pas étudiée. Les effets du fluage, du retrait et de la précontrainte sont pris en considération sous forme de charges équivalentes non-conservatives.

ZUSAMMENFASSUNG

Ein Berechnungsverfahren für die dreidimensionale Rahmenstruktur aus Spannbeton mit Schrägkabeln unter Berücksichtigung des Bauzustandes wird vorgestellt. Ein finites Element wird entwickelt, welches die Effekte der Verwölbung und Biegedrillung eines beliebigen Querschnittes enthält. Die Traglast des Tragwerkes wird nicht untersucht. Die geometrisch nichtlinearen, statischen Analysen während des Bauzustandes und die linearen dynamischen Berechnungen für jeden Zeitpunkt der Konstruktion sind inbegriffen. Die Effekte des Kriechens, des Schwindens und der Vorspannung werden durch nicht-konservative Gleichgewichtskräfte berücksichtigt.

1. INTRODUCTION

In general, prestressed concrete bridges with long spans are constructed by carefully selected construction methods. Most of these construction methods consist of a number of construction steps which normally mean a number of different structural systems during construction. Moreover creep and shrinkage of concrete cause stress redistribution which makes the behaviour of structures more complicated. During the past two decades, a series of efforts to simulate complicated construction methods were made as shown in Table 1, where this study is listed together and compared. [1,2,3,4,5]

The purpose of this paper is to describe the geometric nonlinear analysis procedure of prestressed concrete bridges with flexural-torsion and warping effects implemented in the program SNUBR and present several examples for the validity and applicability.

ANALY -SIS PRO -GRAM	Used Element		Additional degree of freedom		Shape of section	Segmental Creep & Shrinkage Analysis	Geomatric Material nonlinear
	Frame d.o.f	Stay Cable	warping	distorsn			
R M	6	Used				*	
B C	3	Used				*	
SEGAN	8		*	*	1 cellbox	*	
SFRAME	3					*	
SPCFRAME	3					*	G + M
present SNUBR	7	Used	*		arbitrary	*	G

Table 1 Computer Programs for Prestressed Concrete Bridge

2. FINITE ELEMENT ANAYSIS

2.1 General Remarks

A numerical procedure for the geometric nonlinear analysis considering feasible construction stages and linear dynamic analysis at any construction time of three dimensional prestressed concrete frames is presented. This study includes not only the time dependent effects due to load history, creep, shrinkage and aging of concrete and relaxation of prestressing tendons and stay cables but also the flexural-torsional effects including warping in structures with nonsymmetric sections. In the present study tangential stiffness matrices of the elements are obtained using updated Lagrangian formulation based on finite element method. The following assumptions are based.

(1) All materials are linear-elastic.
(2) It is assumed that the shape of a cross section varies only with warping.
(3) Nonlinear terms in shear strains of a frame element are neglected.
(4) Large displacements and rotations and small strains are assumed.

2.2 Stiffness and Mass Matrix

The frame element has two nodes and each node has 7 degrees of freedom including
warping and flexural-torsional effects as shown in Fig.1. The cross section of a
frame element has an arbitrary shape which is represented by 7 sectional
constants and shear center position. The 14 x 14 tangential stiffness
matrix is derived from the
virtual work theorem and 14x14
mass matrix based on
consistent mass is derived
from the energy principle and
variational method. Stay cable
elements are included in the
present nonlinear analysis as
truss elements using Ernst's
equivalent elastic modulus.
Stiffness and mass matrix are
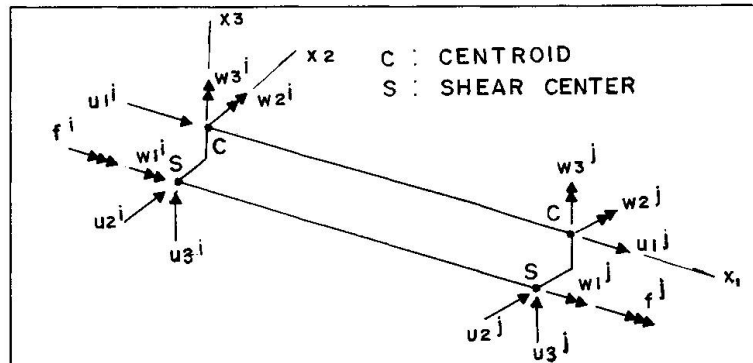also derived by a simillar
method with frame elements.

Fig.1 Displacements of a frame element

2.3 Time Dependent Effects in Concrete Members

The typical time dependent charcteristics of concrete, i.e. creep, shrinkage and
aging are considered in the present study. It is assumed that creep and
shrinkage influence axial deformation, bending deformation, pure torsion
deformation and warping deformation at same time. As creep and shrinkage models
CEB/FIP and ACI model are used which define their own strain behaviour with time
due to loading-unloading stress condition.

The time dependent analysis is based on the superposition principle. The
mathmatical forms of the strain and curvature increments are obtained using
DIRICHLET series using the previous time interval. So equivalent load vector
at each time interval is obtained from the general equilibrium equation of
intitial strains.

2.4 Prestressing Force of a Tendon

The geometry of a tendon within an element is defined by two profiles, i.e. a
cubic curve in the vertical projection plane and a straight line in the
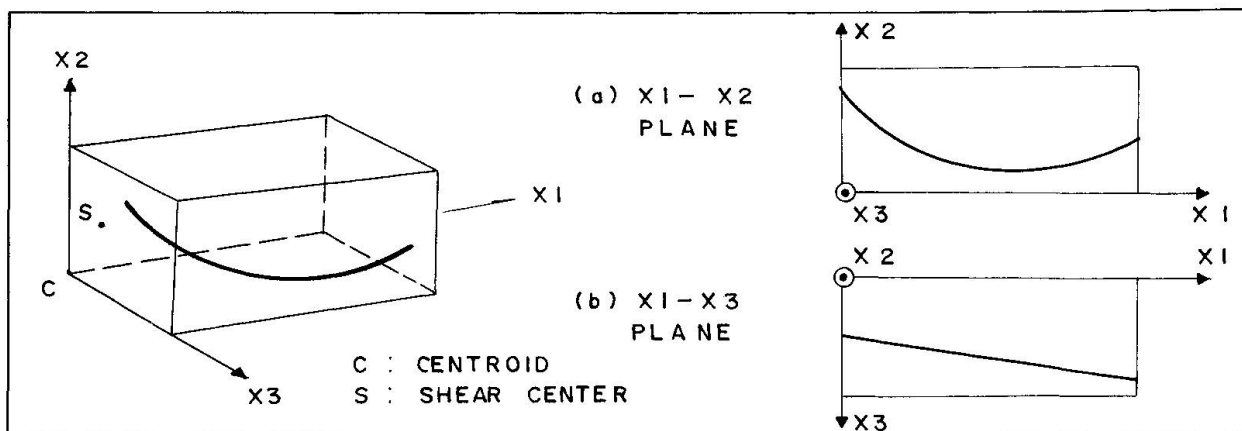horizontal projection plane as shown in Fig.2.

Fig.2 Profiles of a prestressing tendon

The effects of prestressing are considered by the form of equivalent loads. At
the jacking stage, the loads are derived from self-equilibrium equations. The
equivalent loads by the change of the tendon force due to deformation after

jacking are calculated based on the strains of the prestressed members.

The geometric stiffness of the prestressing tendons are considered in the geometric nonlinear analysis. The geometric stiffness of tendons are derived from the deformation and shape functions of main concrete members because the grouted tendons do not have independent shape functions of deformations but are subject to concrete members. After tendons are stressed, the geometric stiffness of tendons are added to the geometric stiffness of a current structure. And then the geometric stiffness of the total structure is not continuous immediately after stressing of tendons because geometric stiffness of a member is embodied from the total sectional resultants.

2.5 Conservative and Nonconservative Loads

In our presentation, the effect of creep & shrinkage and prestressing tendon forces are considered in the form of equivalent loads. The total external loads acting on a structure which are resulted from the prescribed equivalent loads do not keep consistent in the global coordinate system, because the loading directions of these forces would vary according to the relocation of structural members followed by the resulting deformations. Therefore, these forces can be said to be non-conservative. On the other hand, the self-weight of a structure and ordinary loads can be defined as conservative loads because the total external load of them would always keep consistent in spite of structural deformation.

In the case of nonlinear analysis, the unbalanced loads which result in the incremental displacement are found from the difference between the total external loads acting on a structure and the total internal resisting load upto current time-step. Therefore, for the non-conservative forces the total external loads are revised in accordance with the corresponding displacement.

3. DESCRIPTION OF COMPUTER PROGRAM

Program named 'SNUBR' was developed in order to analyze the three dimensional prestressed concrete frame structures according to the presented manner. For the simulation of construction steps, the following "Construction Commands" are defined and directly used for user's input data for the help of a free field interpreter adopted in this program. [6]

(1) Time   (2) Erect
(3) Stress/Remove Tendon   (4) Stress/Remove Cable
(5) Load   (6) Move/Remove Load
(7) Support   (8) Change/Remove Support

Static analysis is carried out according to the successive construction steps simulated by several "Construction Commands" which represent unit construction works and time in days. Each constuction command defines structural system and/or produces unbalanced loads at any time. Tangential equilibirum equations are solved by the combined method, i.e. the tangent stiffness method with the iterative method.

In the case of dynamic anaysis at any construction time, a linear analysis is carried out based on the strucrural geometry and tangential stiffnesses transfered from the current stage. Then the assembled mass matrix of frames and stay cables are calculated. Frequency analysis and/or forced vibration analysis due to a moving concentrated load and general time function loads are carried out. For free vibration analysis, Subsapce iteration method is used and for forced vibration analysis, Mode superposition method and Newmark direct integration method are used.

4. NUMERICAL EXAMPLES

4.1 Natural Frequencies of Thin Walled Beams

To verify the validity of the present stiffness matrix and mass matrix, ten natural frequencies of a thin walled beam with a nonsymmetric section are calculated. The results are compared with the analysis of P.O.FRIBERG who calculated the natural frequencies of thin walled cantilever as shown in Fig.3 including warping derived from VLASOV's differential equations. The difference is about 1.0% as shown in Table 2. [7]

Compression P= 0		Mode	Compression P=1790 N	
By FRIBERG	Present	No	By FRIBERG	Present
31.80	31.80	1	25.01	25.01
63.76	63.77	2	61.28	61.31
137.5	137.8	3	136.0	136.3
199.0	199.1	4	192.4	192.4
278.2	278.6	5	274.9	275.3
483.9	484.6	6	478.5	479.3
556.3	556.4	7	550.7	550.9
657.3	658.3	8	654.8	655.9
767.5	769.2	9	760.8	762.6
1075.	1078.	10	1067.	1070.
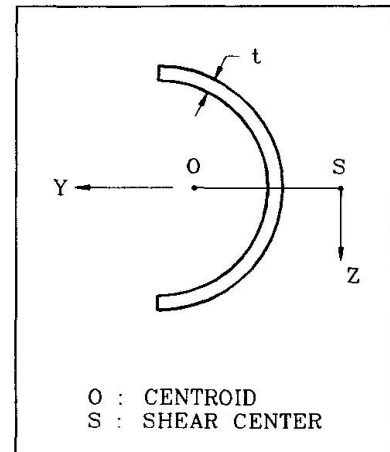
Table 2 Natural Frequencies(Hz)
        of Thin Walled Cantilever

O : CENTROID
S : SHEAR CENTER

Fig.3 Half Circle Cross
      Section

4.2 Dynamic anaysis of P.C. Cable Stayed Bridge

In this example, a cable stayed bridge 80 + 150 + 80 = 310 M long is analysed considering construction steps. Pylon is 40m high above deck and 20m long below deck. For constuction method, free cantilever method is used. And then the influence on natural frequencies and forced vibration are investigated. The change of natural frequencies as time passes are shown in Table 3, where it is found that 1st natural frequency is increased 4 % as time passes and 6 % error can happen in case of neglecting construction steps.

Construction steps	day	NATURAL FREQUENCIES in Hz				Remarks
		1st	2nd	3rd	4th	
Considered	200	0.2414	0.3205	0.5697	0.6624	4%small
	6000	0.2512	0.3251	0.5866	0.6784	1.000
Neglected	200	0.2560	0.3248	0.5818	0.6730	6 % err
	6000	0.2581	0.3275	0.5860	0.6810	3 % err

Table 3 Natural Frequencies of Cable Stayed Bridge (Hz)

For the effect on forced vibration, a moving concentrated load with the speed of 20m/sec (72km/hr) is applied. As shown in Fig.4, dynamic load factor is increased about 3.5% at the center of the bridge.
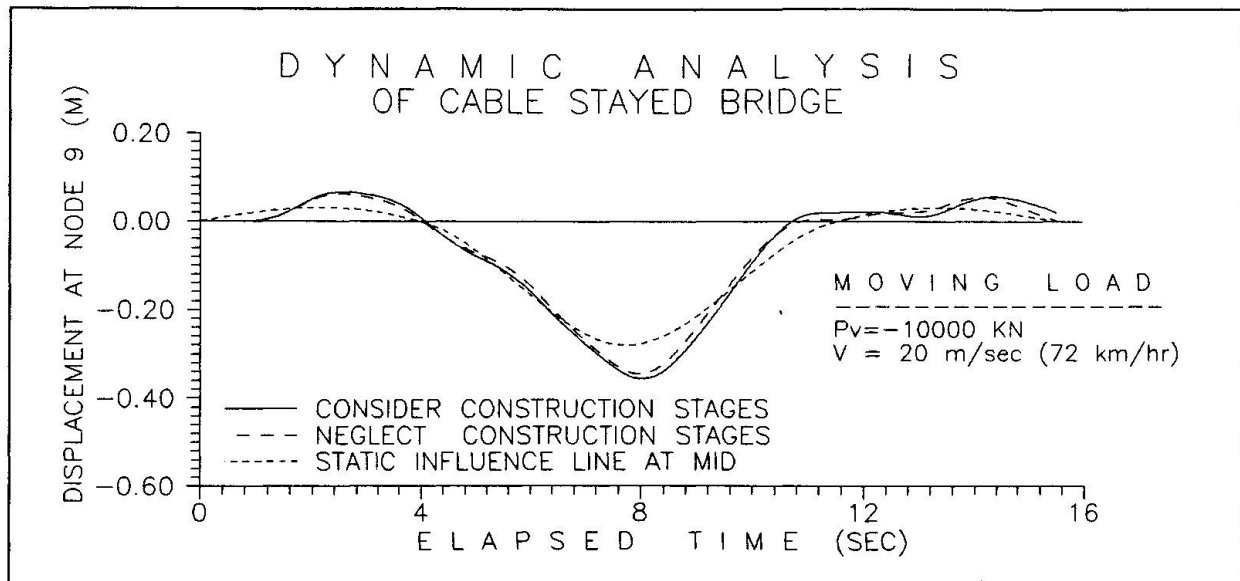
Fig.4 Effect of Moving Load on Cable Stayed Bridge

5. CONCLUSION

A numerical procedure and a computer program SNUBR for the geometric nonlinear analysis considering feasible construction stages and linear dynamic analysis at any construction time of three dimensional prestressed concrete frames are presented. This study includes not only the time dependent effects due to load history, creep, shrinkage and aging of concrete and relaxation of prestressing tendons and stay cables but also the flexural-torsional effects including warping in structures with nonsymmetric sections. Capabilities of the program has been demonstrated by several examples. It can be concluded that the program SNUBR can be useful tool for the analysis and design of segmentally erected prestressed concrete bridges with stay cables.

REFERENCES

1. TECHNISCHE DATENVERARBEITUNG, RM-Spaceframe Maunal, Technische Datenverarbeitung, Heinz Pircher und Partner, 1984

2. EUROPE ETUDES GECTI, B.C. Bridge Construction Computer Program Manual, Europe Etudes Gecti, France, 1977

3. VAN ZYL, S.F., Analysis of Curved Segmentally Erected Prestressed Concrete Box Girder Bridge, U.C.Berkeley, UC-SESM 78-2, 1978

4. M.A. KETCHUM, Redistribution of Stresses in Segmentally Erected Prestressed Concrete Bridge, U.C.Berkeley, UCB/SESM-86/07, 1986

5. KANG, Y.J., SPCFRAME-Computer Program for Nonlinear Segmental Analysis of Plannar Prestressed Concrete Frames, U.C.Berkeley, UCB/SEMM-89/07, 1989

6. WILSON, E.L. and Hoit,M.I., A Computer Adaptive Language for the Development of Structural Analysis Programs, Computer and Structures, Vol. 19, No.3, pp.321-338, 1984

7. FRIBERG, P.O., Beam Element Matrices Derived from Vlasov's Thoery of Open Thin-Walled Elastic Beams, International Journal for Numerical Methods in Engineering, Vol.21 pp.1205-1228, 1985

Lateral Load Behaviour of Large Panel Precast Buildings

Comportement sous charge latérale de bâtiments réalisés avec de grands panneaux préfabriqués

Verhalten von aus Stahlbetonscheiben vorgefertigter Hochbauten unter horizontaler Erdbebenbelastung

Luis E. GARCIA
Partner
Proyectos y Diseños Ltda.
Bogotá, Colombia

Luis E. Garcia is a partner of Proyectos y Diseños Ltda. a Structural Consulting Firm from Bogotá, Colombia. He has been engaged in teaching and research at the Universidad de los Andes. He has been Chairman of the Colombian Building Code Committee and is currently a member of ACI Committee 318.

Mete A. SOZEN
Prof. of Civil Eng.
University of Illinois
Urbana, IL, USA

Mete A Sozen, Professor of Civil Engineering at the University of Illinois, has been active in experimental research related to earthquake resistance of reinforced concrete structures. He is a member of the U.S. National Academy of Science Committee on Earthquake Engineering.

SUMMARY

This paper describes the observed behaviour of a large panel concrete precast building under simulated seismic loads and its mathematical modeling. This mathematical model, calibrated by a series of static tests, was used to study the dynamic response of the structure for different types of earthquake motions.

RÉSUMÉ

Cet article décrit le comportement d'un édifice réalisé avec de grands panneaux préfabriqués soumis à un séisme simulé, ainsi qu'à sa modélisation mathématique; celle-ci étalonnée par une série d'essais statiques, a été exploitée pour étudier la réponse dynamique de la structure pour divers types de mouvements pouvant être provoqués par un tremblement de terre.

ZUSAMMENFASSUNG

Dieser Bericht beschreibt das Verhalten von grossen Stahlbetonscheiben vorgefertigten Hochbauten unter der Einwirkung von seitlichen Erdbebenlasten und das sich daraus ergebende mathematische Modell, das aus einem 1:1-Versuch hervorging. Dieses Modell wurde erweitert, um auch Antwortspektren verschiedener Erdbeben abzudecken.

1. INTRODUCTION

An insight into the behavior of large panel precast reinforced concrete buildings under lateral loading and its mathematical modeling has been obtained through a series of full scale lateral load tests on a five story large panel precast building. The static lateral loads simulated the distribution the inertial forces during an earthquake. Mathematical models were developed before the tests, which were subsequently calibrated using the actual test results. This models were extended to cover the behavior under seismic actions, which led to definition of behavior patterns under different types of earthquakes [1]. The building tested was very lightly reinforced and represented the type of precast construction used in the Republic of Colombia before the enactment of the Colombian Code [2]. In addition the building was not connected with tension reinforcement to the foundation.

2. EXPERIMENTAL PROGRAM

2.1 Precast Building Tested

The full scale precast building tested was a five-story low-rise apartment building with an area per floor of 157,64 m^2 as shown in Figure 1. The clear height of the precast panels was 2,20 m and the floor slabs had a thickness of 250 mm. The total height of the building was 12,25 m (Figure 2). The total mass of the building was 460 metric tons. All continuity reinforcement was located and welded in the gaps between precast elements. These gaps were filled later with grout. All the precast panels were 80 mm thick. The internal reinforcement of the panel did not extend from the borders of the panel. Each panel had horizontal bars that extended into the vertical connection. One 9,5-mm diameter vertical reinforcing bar was located in all vertical joints between panels. All 63 vertical joints between precast panels had vertical reinforcement; but only in 24 of them it was continuous from floor to floor. No vertical reinforcement was anchored to the foundation. The building was, therefore, very lightly reinforced having only 24 bars with a 9,5 mm diameter from top to bottom without any connection to the foundation. All floors, including the roof, were made up of plant precast steam cured elements. The edges the floor elements had connecting reinforcing bars that were welded to similar bars in the neighboring elements, achieving the continuity needed to obtain a floor diaphragm effect.

2.2 Test Setup and Procedure

Lateral loads were applied from the reaction frame to the precast building using high-strength steel cables attached to hydraulic rams. Two rams per floor were used. Applied loads were measured with twenty load cells, one at each ram. Lateral deflection measurements were obtained using extension bars that recorded the drift (relative lateral deflection) between floors. Each extension bar was provided with a 0.001-in mechanical dial gage. Horizontal and vertical base movements were obtained with additional mechanical dial gages. Ambient vibration records were made, before and after each series of lateral load applications.

2.3 Earthquake Simulator Friction Tests

A series of static and dynamic tests [3], with the dynamic tests including two different types of earthquakes, were performed as part of the research project on the earthquake simulator of the Católica University in Lima, Peru. The prototypes were designed to have normal contact stresses in the same range of those found in the horizontal joints of the precast building. The observed static friction coefficient ranged from 0,65 to 0,68. The dynamic friction coefficient observed in the harmonic tests varied from 0,71 to 0,73. In the seismic tests a value of 0,78 was obtained. Based on this, for the evaluation of the experimental tests performed on the precast building a value of 0,66 was used.

3. EXPERIMENTAL RESULTS

3.1 Base Shear

Seven lateral load tests were performed on the structure from July to September of 1989. These tests are named 0, A, B, C, D, E and F. Table 1 gives a summary of the direction of loading of each test, the maximum static base shear reached, V_{max}, in kN and the value of the seismic coefficient, C_S, defined as $C_S = V_{max}/W$, where W is the active lateral load mass (W = 437 metric tons). Test 0 corresponds to first cracking of the building in the E-W direction. Test B corresponds to the first time the lateral load strength of the building was reached in the E-W direction, obtaining a seismic coefficient of 37,9% of the mass of the building, value that was surprisingly high for a building so lightly reinforced and disconnected from the foundation. Test C correspond to the only test that was performed in the N-S direction and it did not reach the strength of the building although a base shear of 37,3% of W was measured. With Test E the lateral strength of the building was reached in the opposite direction (W-E) of Test B. A value of C_S of 41% of W was measured. Test F was performed to obtain the reduction in stiffness of the building after having reached twice the lateral load strength.

3.2 Measured Deformations

A large decrease of stiffness was observed for the two tests that reached the strength level in the E-W direction (Test B) and then in the W-E direction (Test E) as the roof deflection reached in Test B was 16,5 mm for a base shear of 37,9% of the mass of the building, compared with 90,6 mm for a base shear of 41% of the mass of the building. It is note worthy that only for Test E the story drift in two of the floors was greater than 1% of the story clear height. For Test E the graph of story shear vs. story drift is presented in Figure 3. From these graphs it is evident that the structure went well into the inelastic range.

3.3 Observed Cracking

During Tests 0 and A, no cracking due to the applied lateral loads was observed. During Test B the first cracks in the vertical joints between precast panels were observed. These cracks extended as the lateral load was increased. Then the first cracks in the top horizontal joint of the panels appeared in the north and south exterior walls of the western sector of the building. These horizontal cracks had extended to all the building before the strength level was reached. No internal cracks in the precast panels were observed, with the exception of panels with window openings. During Test C, the only one in the N-S direction, no cracking was observed, different form that caused from the previous tests. The same is true for Test D. For Test E there was a notorious increment of the width of the vertical cracks in the vertical joint of the precast panels. There were interior cracks in some of the panels. Notorious work in the horizontal joints with vertical continuous reinforcement caused by sliding of the joint was observed.

4. INTERPRETATION OF OBSERVED BEHAVIOR

The cracking sequence was: (a) Fine cracking was observed in the vertical joints between panels (C_S=25,6%). (b) The cracks extended and increased in width as more lateral load was applied. (c) The first cracks at the top horizontal joint of the panels appeared at the third floor of the West side of the precast building at a C_S of 32,1% of W. (d) The cracks at the top joint of the panel had appeared in all of them when the C_S reached 35,7% of W. The load was applied from East to West and the first horizontal cracks appeared in the West zone of the building, where the overturning moment introduces compression. These means that the cracks were not caused by flexural induced tension; they were caused by roll-over (overturning) of the precast panels. This interpretation was confirmed by the mathematical modeling.

5. ANALYTICAL MODEL

The analytical evaluation of a large panel structure has been performed traditionally assuming that the structure is monolithic. The internal stresses are then obtained from a linear elastic analysis and strength for the elements and their connections are provided for these stresses. A "box effect" is present due to the non planar connection between precast elements thus forming a three dimensional structure. Large differences between the theoretical behavior and the one encountered in tests due to the use of planar analytical models.
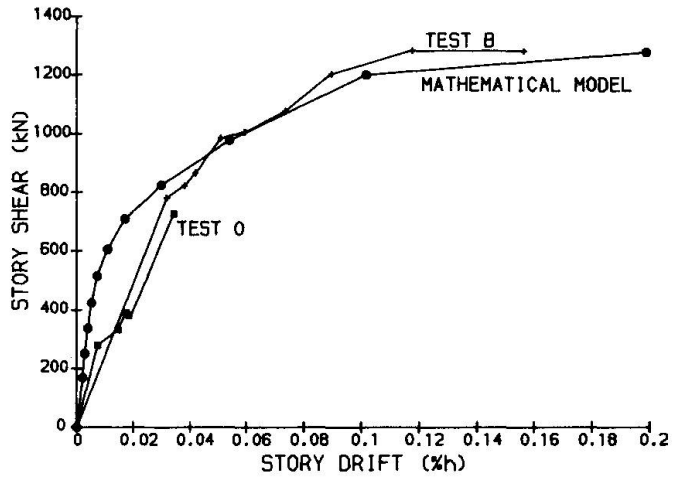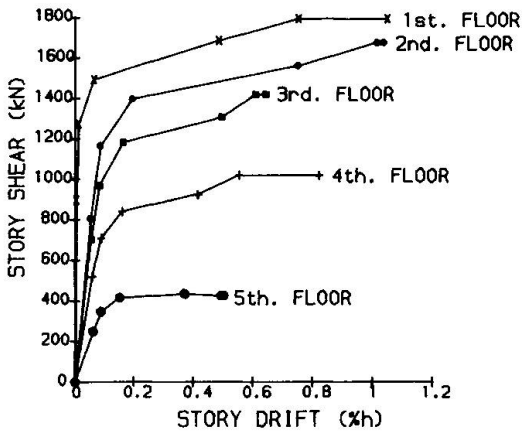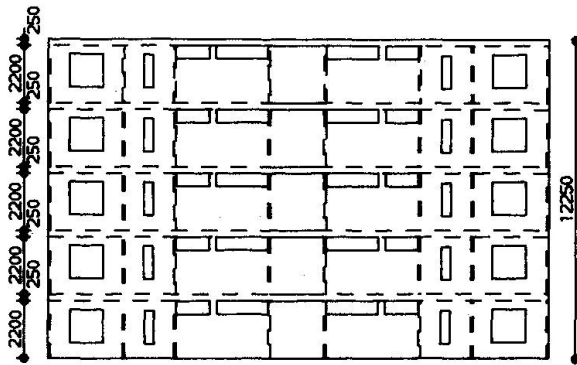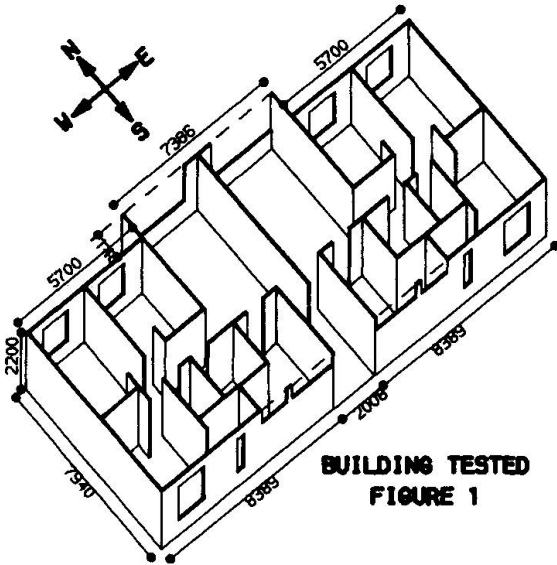
An analytical model appropriate for describing the behavior observed during the experimental tests of the building was developed before the tests were carried out and was subsequently calibrated using the experimental results. The model takes into account the non-linear response of the structure by modifying the stiffness of the different elements as they are stressed by the lateral load. A procedure of successive linear stages was adopted to describe the general non linear behavior. The analysis is initiated with a monolithic structure. With the results of this analysis the possible modes of failure of the elements and their connections are evaluated and the one that occurs at a lower lateral load level is taken as critical. The properties of the critical element or connection involved are then modified. The level of lateral load and deflection obtained are recorded and a new linear elastic analysis is performed where a new evaluation is performed, giving a new critical element or connection. This procedure is repeated until loss of equilibrium is detected. The modes of failure that are verified correspond to: (a) sliding of the horizontal connection, (b) overturning of the panel, (c) cracking and sliding of the vertical connection between panels, (d) internal shear failure of the panel, and (e) yielding of the vertical continuity reinforcement. The results obtained with this mathematical model correspond to the first lateral loading of the building. Figure 4 shows, for the E-W direction, the results obtained for the third floor as compared with the measured experimental results of the same floor for Tests 0 and B. The agreement of the results is significant and the same is true for all the other floors.

6. DYNAMICAL RESPONSE IN THE INELASTIC RANGE

Using the program presented in [4] and linear idealizations of the relations between story shear and story drift obtained from the experimental lateral load tests of the precast building, the response of the building to base excitation representing strong ground motion corresponding to different soil conditions was obtained. A parametric study of the dynamic response was performed for cases that included: (a) variations of the hysteretic characteristics, (b) different levels of lateral stiffness of the structure, (c) earthquake records with different types of soil conditions, (d) peak ground acceleration of the earthquake records, (e) effects of damage accumulation caused by the structure being subjected to several successive earthquakes, and (f) an earthquake acting in a direction at an angle with the principal plan directions. Records obtained in El Centro (1940 Imperial Valley Earthquake), Castaic (1971 San Fernando Earthquake), Wilshire (1971 San Fernando Earthquake), Viña del Mar (1985 Chile Earthquake), Miyagi (1978 Japan), and Mexico City (1985 Mexico Earthquake) were used.

From the observed damage during the static tests of the precast building, bounds for the response were established. These bounds were a story drift of 4 mm for minimal damage and a story drift of 24 mm for the threshold of life threatening damage.

The effect of the peak ground acceleration is shown in Figure 5, where the maximum story drifts are plotted against peak ground acceleration of the earthquake records. Only those cases where the stiffness of the structure was reduced to one half and one quarter of the initial stiffness have story drift beyond the 24 mm limit. With the soft soil records (Mexico and Miyagi) the maximum story drift obtained was 1,2 mm, well into the minimal damage zone. For damage accumulation, three successive application of the full El Centro record, showed for the third application a maximum story drift of 24,3 mm.

BUILDING TESTED
FIGURE 1

ELEVATION
FIGURE 2

MEASURED STORY DRIFT
TEST E
FIGURE 3

MATHEMATICAL MODEL RESULTS
THIRD FLOOR
FIGURE 4
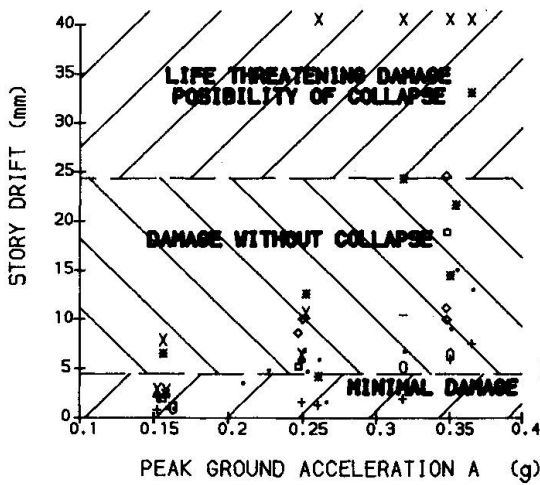
· EW — Full Stiffness
+ NS — Full Stiffness
* EW — 1/2 of Full Stiffness
0 NS — 1/2 of Full Stiffness
X EW — 1/4 of Full Stiffness
⁻ NS — 1/4 of Full Stiffness
◇ EW — Acumulated Damage
□ EQ Direction N45°E

MAXIMUM STORY DRIFT AS A FUNCTION
OF THE PEAK GROUND ACELERATION
FIGURE 5

7. CONCLUSIONS

A full scale very lightly reinforced large panel precast building was subjected to seven lateral load tests obtaining base shear strengths of the order of 3/8 of the mass of the building and load deflection responses that exhibited a non fragile capacity. Even though the building was not connected to its foundation this did not affect the static lateral load strength of the building. It was possible to explain the failure mechanisms of the building and to establish analytical bounds of response under lateral loads. The static and dynamic friction tests of concrete surfaces cast at different moments gave an insight of the friction phenomena and permitted the development of an analytical model for the response of this type of structures to base excitations representing strong ground motion. Using the dynamic analytical model it was possible to confirm that ground motions rich in short vibration periods tended to affect the building more than motions rich in long periods as encountered in earthquake records from soft soil sites.

The observed behavior in the tests and the results obtained from the analytical models could serve as a basis for future performance requirements [5] and guidelines for analysis methodologies [6] for seismic loading for large-panel precast buildings.

REFERENCES

1. INDUSTRIAL DE CONSTRUCCIONES S.A., "Full Scale Test of a Five Story Large Panel Precast Building under Lateral Load and its Interpretation", Proyectos y Diseños Ltda. and Igeniería Técnica y Científica Ltda., Bogotá, Colombia, December 1989, 243 pp.

2. - MINISTRY OF PUBLIC WORKS AND TRANSPORTATION, "Colombian Seismic Code CCCSR-84" (in Spanish), Decree 1400 of June 7 of 1984, Bogotá, Colombia, June 1984, 307 pp.

3. BARIOLA, J., "Dynamic Friction Coefficient in Reinforced Concrete Structures" (in Spanish), Lima, Perú, October 1989, 39 pp.

4. SCHULTZ, A. E., "An Experimental and Analytical Study of R/C Frames with Yielding Columns", Doctoral Dissertation, Graduate College, University of Illinois, Urbana, Il., 1985.

5. BREEN, J.E., "Why Structural Concrete", IABSE Colloquium "Structural Concrete", Sttutgart, 1991.

6. SCORDELIS, A., "Analysis of Structural Concrete Systems", IABSE Colloquium "Structural Concrete", Sttutgart, 1991.

TABLE 1
SUMMARY OF THE STATIC EXPERIMENTAL LATERAL LOAD TEST

| TEST	-0-	-A-	-B-	-C-	-D-	-E-	-F-
Direct.	E-W	E-W	E-W	N-S	W-E	W-E	W-E
c_g	0,209	0,151	0,379	0,373	0,210	0,410	0,284
V_{max}*	913	660	1655	1630	918	1793	1241

* V_{max} in kN

Urban Interchanges on Elevated Structures

Echangeurs routiers en milieu urbain

Neuartige Kreuzungen innerstädtischer Hochstrassen

Vijay CHANDRA
Vice-President
Parsons Brinckerhoff
New York, NY, USA

George SZECSEI
Prof. Assoc.
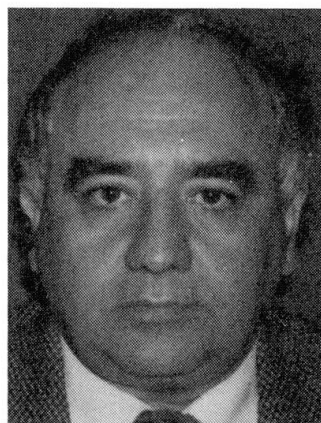Parsons Brinckerhoff
New York, NY, USA
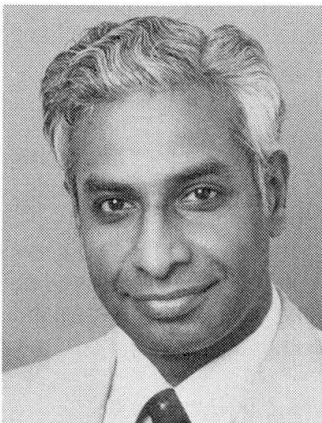
Vijay Chandra, P.E., vice-president and senior professional associate at Parsons Brinckerhoff, a leading US transportation design firm, has directed the structural design of several award-winning bridges, and is a member of the PCI Bridge Committee.

George Szecsei, P.E., professional associate at Parsons Brinckerhoff, has been project engineer on several award-winning bridges. He has co-authored several papers with Vijay Chandra.

SUMMARY

This paper illustrates the design and construction in Phoenix, Arizona, of a novel type of urban interchange on elevated structures. This approach can often be implemented at a lower cost and on smaller sites than traditional multilevel interchanges.

RÉSUMÉ

Cet article illustre la conception et la construction à Phénix, Arizona, d'un nouveau type d'échangeur routier en milieu urbain, situé au-dessus de structures élévées préexistantes. Cette approche peut souvent s'appliquer de façon plus économique et sur des surfaces plus restreintes que les solutions traditionnelles d'échangeurs à plusieurs niveaux.

ZUSAMMENFASSUNG

Dieser Vortrag behandelt den Entwurf und die Konstruktion neuartiger Kreuzungen innerstädtischer Hochstrassen. Diese Lösung kann oft mit geringeren Kosten und mit geringerem Landverbrauch als bei den üblichen mehrstöckigen Kreuzungen erreicht werden.
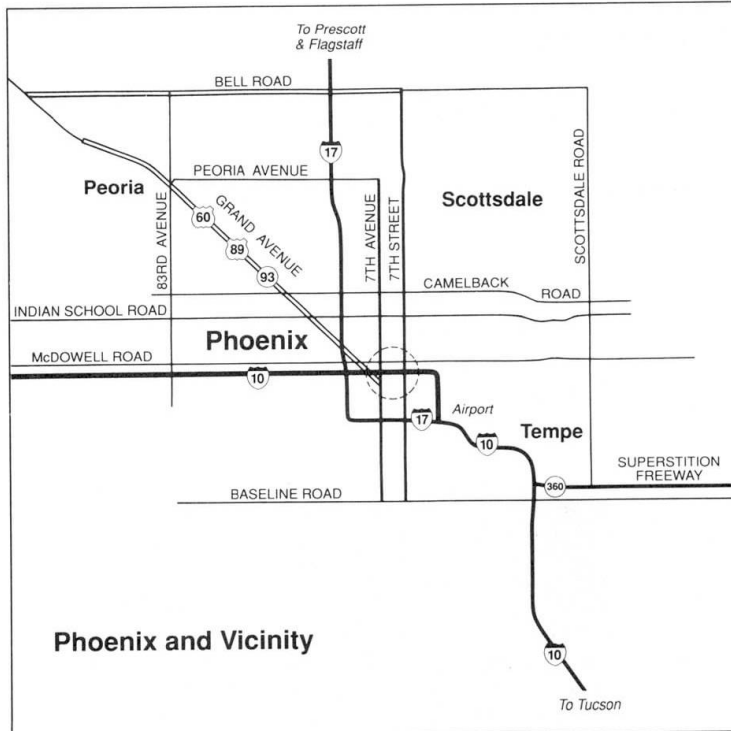
Figure 1. Site Location

Figure 2. Bird's eye view (Seventh Avenue)

INTRODUCTION

In Phoenix, Arizona, two prestressed concrete interchanges of complex geometry have proved an appropriate structural solution for compressing highway structures into the cramped urban landscape. The elevated structures, linking the north-south arterials Seventh Street and Seventh Avenue to the new depressed highway I-10, are neither full multilevel elevated interchanges with on/off ramps on independent structures, nor completely ground level interchanges. They are in essence compact urban interchanges that have been partly elevated, with certain ramps compressed right into the main structure to reduce the ordinary four levels of an elevated interchange to two.

This paper examines the choices of analytical approach and of construction methods that made rapid (one-year) design and construction possible despite the complexity: finite element analysis of the structures, and postprocessing of results into formats directly useful to engineers.

At these sites, where I-10 was to be connected through the heart of metropolitan Phoenix (Fig. 1), right-of-way could be costly, and lengthy construction disruptive. The Arizona Department of Transportation therefore favored an urban interchange over a multilevel interchange. It was found, however, that the scarcity of land would force the ends of certain ramps to fall *on structure*, with motorists executing their turns on the structure itself (Fig. 2).

MAKING THE INTERCHANGE CONCEPT WORK

Fusing into the main structure four of the usual eight on/off ramps achieved compactness, but at the cost of generating ramp-structure interactions that challenged analysis. The ramps rest on curving projections of the mainspans, making a flared shape, wider at the abutments to accommodate the ramps (Fig. 2). Each structure would look from above like an hourglass, wide at the abutments and narrow at the central pier—the waist of the hourglass. The concept was simple, but the design and construction of such unusually shaped structures would not be.

What makes the urban interchange on structure so complex for design and analysis is the interactive load transfer among all these parts that rest on one another. The loads of the four curved and skewed prestressed concrete ramps, for example, would have to be transferred onto the prestressed concrete mainspan late in construction—when a small error might easily make a ramp rotate from its own weight instead of uniformly sitting on the bearings. The interactive stresses of the entire odd-shaped concrete structure would have to be understood at each stage of construction and load transfer if the structures were to survive the hard-to-predict stresses of their own construction. The final simplicity would be achieved at the price of a major analytical effort, individualized at each of the two sites.

UNUSUAL STRUCTURES/UNUSUAL ANALYSES

Unusual structures require unusual analysis techniques. State-of-the-art finite element technique with up to 2,000 elements of various shapes was employed to model the structures, and greatly assisted in understanding the interactive stresses and the true behavior of the ramp structures with their extreme skews.

The main part of the structures at both locations is a two-span continuous post-tensioned concrete structure supported on concrete abutments at both ends and supported through the midsection by concrete columns erected in the median of I-10. The curved ramp structures are of concrete box section, each of a different length and different skew to the main structure (Fig. 3). The portion that is on structure rests at one end on a protrusion on the side of the main structure (Fig. 4). The triangular gaps resulting from the peeling off of the ramps from the main structure in front of the abutments also had to be covered—to support landscaping in these visually important spots. Both structures included separate pedestrian walkways, with ramps for disabled persons.

In part, the design was driven by aesthetic needs, and planned to be visually pleasing for users and neighbors alike. Seen from above it flares out like a great concrete hourglass, wide at the ends. Seen in profile by I-10 motorists, its notched curves arc powerfully against the sky. Driving up the ramps, motorists discover landscaping high above ground level, thanks to hidden structural elements that take the weight of earth and plants.

To meet our aesthetic goals, we streamlined the fascia to present a smooth, aesthetically pleasing appearance to the travelling public on I-10, with canopied fences that offered smooth transitions at their ends and at the intersections of the ramps and the main structures. Even landscaping requirements affected structural design: the final landscaping decision to plant shrubs into the triangular areas formed between the ramp structures, main structure, and abutments was not a decision calculated to make life easy for the structural designer. We would need to support a layer of soil at least a foot deep and accommodate a maintenance
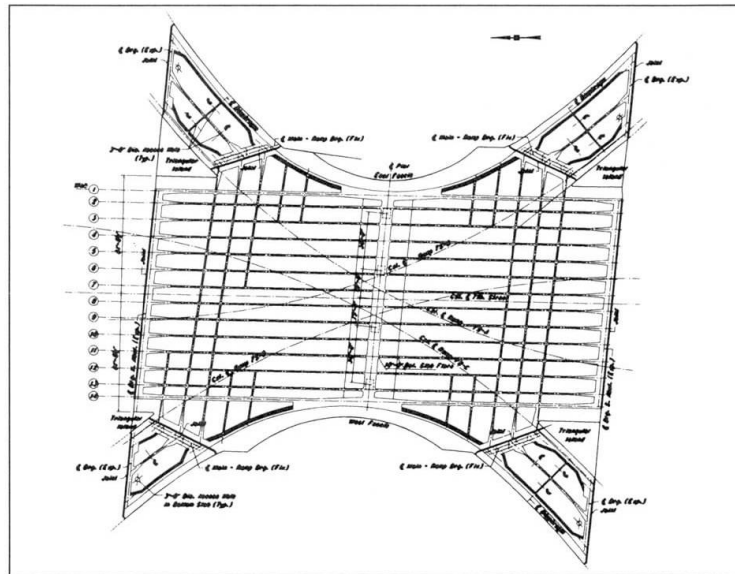

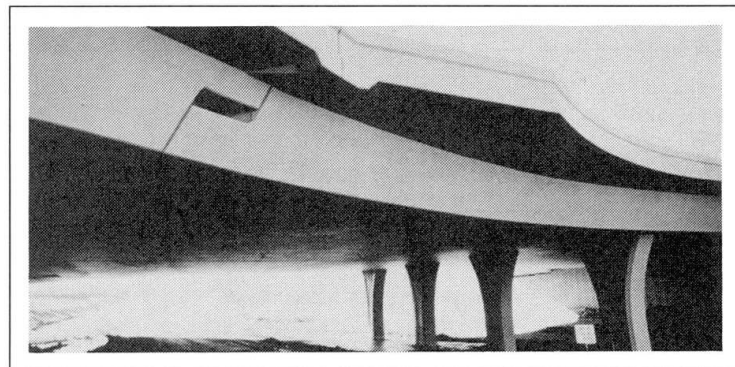**Figure 3.** Typical framing (Seventh Street)

Figure 4. Ramp (left) sitting on the main structure (right)

THE STRUCTURES AT A GLANCE		
	Seventh Street Structure	**Seventh Avenue Structure**
Main Structure		
-Span lengths ft	121' & 121'	141' & 129'
-Width ft	260' & 280' at abutment & 125' at piers	360' & 400' at abutments & 130' at piers
-Type	Cast-in-place post-tensioned concrete with curved fascia	Cast-in-place post-tensioned concrete with curved fascia
Ramp Structures		
-Span lengths ft	Vary, 60'-85'	Vary 110'-170'
-Width ft	32'	32'
-Type	Cast-in-place curved reinforced concrete	Cast-in-place curved post-tensioned concrete
Foundation		
	Spread footings on S-G-C (sand, gravel, and cobbles) material	Spread footings on S-G-C material
Triangular areas		
	Cantilever slabs with 29' max. overhang	Cantilever slabs with 27' max. overhang coupled with pretensioned concrete beams

vehicle live load right in the gap between structures. Bridging this gap to support that load threatened to create major structural problems by imposing heavy loads on the ramps. By cantilevering the abutment wall up to about 25 feet, however, much of the triangular area load was relieved off the ramps and transferred directly to the abutments. At Seventh Avenue, the cantilevering alone was insufficient to cover the entire triangle, and the gap beyond the cantilevers had to be covered using precast concrete elements. Before placing the fill for landscaping, we waterproofed the top of the cantilever and precast elements.
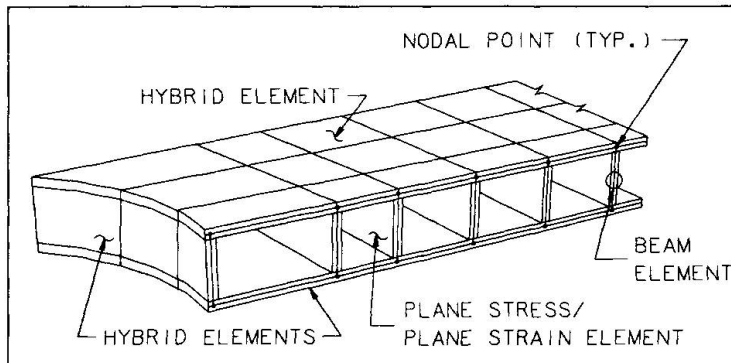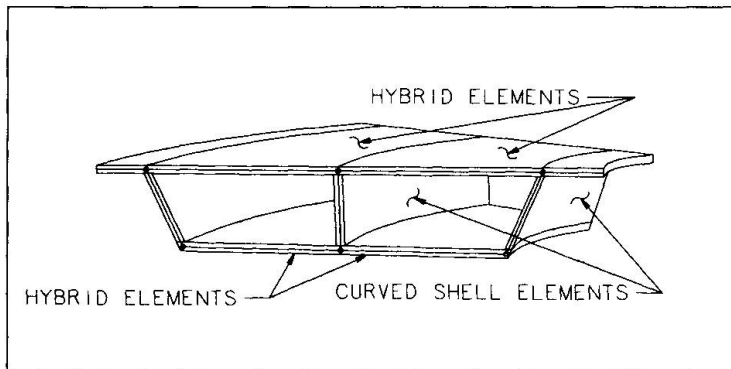

Figure 5. Finite elements of main structure

Figure 6. Finite elements of ramps

FINITE ELEMENT APPROACH

The Seventh Street and Seventh Avenue structures were similar in concept but would have to be analyzed independently because of their unique shapes, geometric nonsimilarities, ramp-structure variations, span length variations, etc. What mathematical modeling method we chose for all this analysis might well determine what questions we could ask effectively.

Surveying the available methods, we closed in on two finalists. The space grid method simplifies the structure into a Tinkertoy-like skeleton of lines and nodes; the finite element method has similar nodes, but connects them by surfaces instead of lines. Thus a real three-dimensional beam would be represented as either a single line (space grid) or as a set of surfaces, as if boxing-in the beam (finite element).

Before embarking on the most appropriate method, we critically compared the two candidate methods as to their ability to reflect the true behavior of such difficult features as transfer of torsional loads, transverse stress distribution, temperature gradient, post-tensioning forces, skewed ends, and curved surface areas. The evaluation showed the finite element procedure to be superior.

Before applying the finite element concept to the entire structure, we evaluated discrete structural models for the various element shapes and applied loads. Once a 'level of comfort' was achieved, the full-structure model was pursued.

The main structure required about 1,700 finite elements for the Seventh Avenue structure and 1,400 finite elements for the Seventh Street structure. Each of the ramp structures was individually analyzed and required about 160 elements. The types of elements were quite varied, including trapezoidal and triangular hybrid for slabs, diaphragms, and curved fascia webs of the main structure; curved shell for webs of ramps; and plane-stress/plane-strain for the longitudinal webs of the main structure. Beam elements were introduced between adjacent plane-stress/plane-strain elements (Figs. 5, 6).

Transient loads, such as live loads, were applied on the top slab as surface pressures. After careful evaluation of alternative modeling approaches, post-tensioning loads were applied as equivalent loads using the parabolic curve approach along the webs and concentrated loads at the ends of the elements. The vertical, lateral, and axial components of the post-tensioning forces were input.

In order to fathom the finite element run output in easy-to-understand terms, we developed a postprocessing program that reduced the stresses at any particular nodal point to shear and moment forces. This proved a tremendous help in verifying the behavior of the structure.

DESIGN OF PERIPHERALS

The principle that unusual structures exhibit unusual behaviors affects not only the design of the structure itself, but also the design of such important peripherals as bearings and deck expansion joints. Each of the peripherals had to be carefully evaluated, and systems selected and designed to function properly within these unusual structures.

Pot bearings were selected, as they provided multidirectional rotational capability. The bearings were designed incorporating the direction and amount of thermal movements, axial shortening during post-tensioning, shrinkage, and creep given by the finite element analysis, together with AASHTO seismic requirements. To spare the bearings from having to resist high transverse earthquake forces, side shear walls at the two abutments provided the resistance.

A special issue in bearing selection was the presence of uplift forces at the center bearing because the ramp structures were so long and transversely stiff at the bearing lines. In a first attempt to control this, the hinged-end articulated diaphragm was optimized for the gravity loads. However, this proved difficult from the viewpoint of thermal loads, making uplift bearings necessary.

Bearings had to be accessible for inspection and replacement if necessary. At the abutment, the access is easy from below

Figure 7. Typical ramp section

Figure 8. Cross-section through bearing inspection chamber

Figure 9. Typical ramp cross-section

the structure, but at the hinges, where the ramps sit on the main structure, the access requirements imposed a design challenge. We met it by providing entrance to the ramps through an access manhole at the ramp soffit and through ports in the ramp hinge articulation (Figs. 7, 8, and 9).

Deck joints, too, needed careful attention since the unusual shape of these structures imposed unusual movements on the deck joints. Finite element analysis indicated that thermal, creep, shrinkage, and post-tensioning movements would be severe both transversely and longitudinally. After evaluation, a strip seal deck expansion joint was selected as providing the necessary movements in two directions.

CONSTRUCTION

No design is complete if the designer, who knows all the problems and concerns in the design of such complex structures, does not communicate those concerns to the contractor and field engineers. This is especially critical where a particular design is bid by several contractors. Giving the contractor a suggested detailed sequence of construction is helpful. Our design did not try to dictate a construction method, but opened the door for the contractor's initiative by incorporating in the construction documents a suggested sequence of construction together with notes that highlighted the designer's concerns at various stages. It proved very beneficial; contractors for both structures mostly used the suggested methodology—with some improvements, which were acceptable to us.
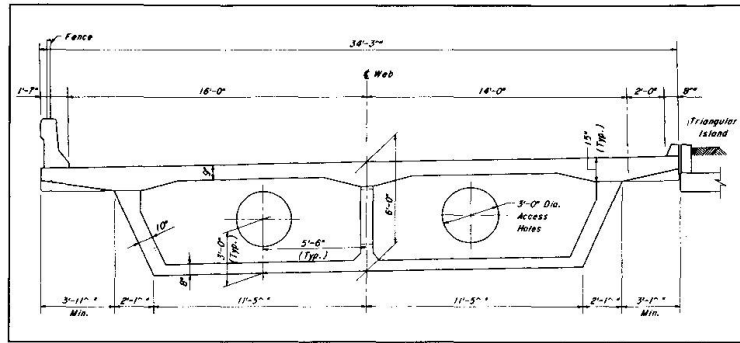
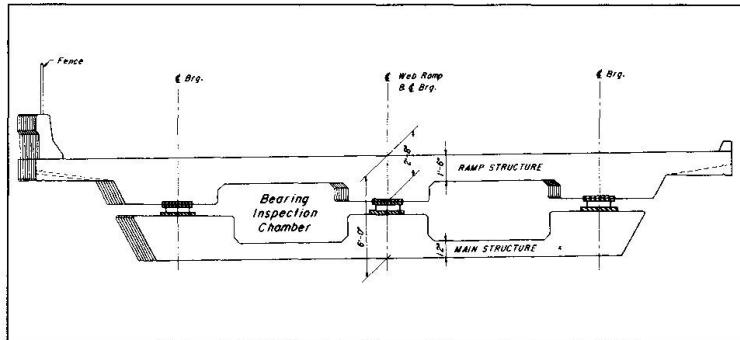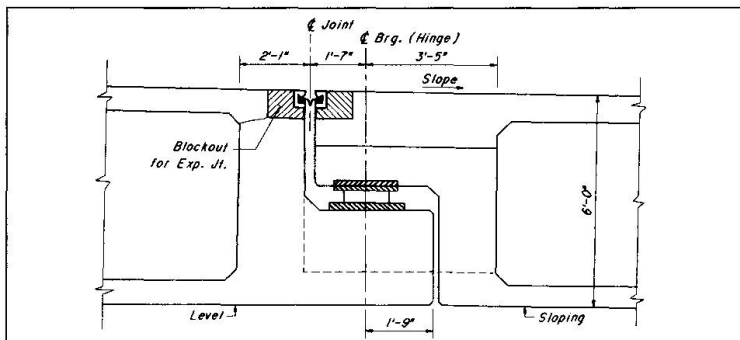Close coordination between the designer and the contractor is a must: both benefit from the interaction, and this experience benefits their future projects as well. On these two projects, such cooperation was realized to be essential, and with the timely cooperation of the client, problems as they were perceived and encountered were solved to every party's satisfaction.

In Arizona, most concrete box girder superstructures are poured directly on a 'mud slab' as the base form. The mud slab is a thin unreinforced concrete slab poured to grade on a stabilized fill (the 'mud'). Both these projects benefited from the method, which allowed pouring the deck slabs without recourse to the scaffolding commonly used in other regions.

CONCLUSION

However difficult the analysis and design, the concept of an urban interchange on structure has proved quickly and economically constructible. The $2.6 million Seventh Street structure ($62/square foot) and the $3.6 million Seventh Avenue structure ($63/square foot) were each built in about a year, and cost considerably less than comparable multilevel interchanges.
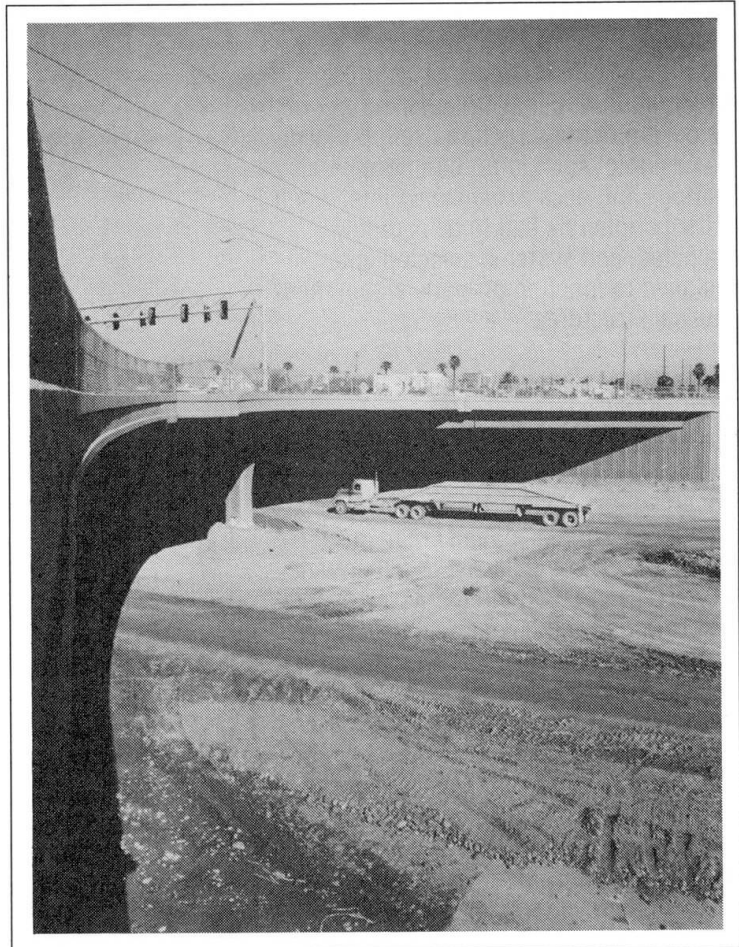

Figure 10. A driver's view from I-10 (Seventh Avenue)

Phoenix's new urban interchanges on structure, and the design and construction that made them possible, offer a new option for cities seeking to thread highways and interchanges through the already dense urban fabric (Fig. 10).

CREDITS

Client
Arizona Department of Transportation

Managing Consultant
Howard Needles Tammen & Bergendoff

Structural Engineer
Parsons Brinckerhoff Quade & Douglas, Inc.

Contractors
Tanner Construction (Seventh Street Structure)
McCarthy Construction (Seventh Avenue Structure)

Portions of this paper appeared, in different form, in *Civil Engineering* (September 1988), published by the American Society of Civil Engineers, and are reused here with their permission. These structures have received engineering awards from the American Concrete Institute (Arizona), Post-Tensioning Institute, and American Consulting Engineers Council (Arizona).